AN INVESTIGATION OF EVANESCENT WAVE EXCITATION OF FLUORESCENCE USING OPTICAL FIBRES

by

Colin E. Potter B.Sc.(Hons)

A thesis submitted to
Dublin City University
for the degree of

Master of Science

Supervisors: Dr.V.Ruddy & Dr.B.MacCraith

School of Physical Sciences
Dublin City University
Ireland

October 1990

Declaration

This thesis is based on my own work

DEDICATION

This work is dedicated to my Mother and Father, two sisters Jane and Susan, my brother Ian, and also to my very special friend Audrey.

A special dedication to my late friend Ian Travers, a fellow climber, - without whom I would never have achieved so much.

CONTENTS

CONTENTS (contd.)

AN INVESTIGATION OF EVANESCENT WAVE EXCITATION OF FLUORESCENCE USING OPTICAL FIBRES

COLIN E. POTTER

ABSTRACT

A study of fluorescence excited by the evanescent wave (E.W.) of guided radiation in an optical fibre is reported. E.W. excitation of fluorescence is important because of its application in novel optical sensors for biomedical and chemical parameters.

An experimental system whose design is based on the theory of evanescent wave (E.W.) excitation of fluorescence is described. Several chemical immobilisation techniques for the attaching of fluorescent dye molecules onto the surface of an unclad optical fibre core were investigated and were found to be unsatisfactory. These techniques when examined using evanescent wave excitation lacked consistency with regard to their optical emission spectra, peak wavelength and intensity of fluorescence.

A novel technique to coat an unclad optical fibre core surface with a porous glass coating (a Sol-gel) which was doped with fluorescent dye was investigated and found to have potential in the area of optical fibre sensors. Fluorescent dyes such as fluorescein, fluorescein isothyocyanate and rhodamine 6G were used as initial dopants within the Sol-gel matrix. Using the technique of evanescent wave excitation the fluorescent dyes were found to exhibit emission spectra comparable to that of bulk excitation.

A pH probe was constructed using a fluorescein-doped Sol-gel coating around a short length (90mm) of unclad optical fibre. It was found to have a pH sensitivity in the range of pH2 to pH7 and a response time of approximately 5s.

CHAPTER 1

FIBRE OPTIC FLUORESCENCE SENSING

1.1 Introduction

In the mid 1800's an Irish physicist John Tyndall demonstrated the concept of guiding light using a jet of water as a simple waveguide. Since then the concept of guiding light has been developed into modern optical fibres. There are two main areas in which optical fibres are used, communications and sensing. Using the inherent qualities of optical fibres such as resistance to corrosion and immunity to electromagnetic interference, optical fibres can be used to sense such parameters as temperature, pressure, acceleration and flow of liquids and gases. Some such sensors are now commercially available [1].

A sensor is a device that is able to indicate continuously and reversibly the concentration of an analyte or a physical parameter. Optical fibre sensors offers many advantages over other methods of sensing. For example,

1. Optical sensors do not require a reference signal as is required by most electrical methods of sensing such as potentiometric methods.

2. The ease of miniaturisation allows the development of very small and low weight fibre sensors.

3. Analysis can be performed in almost real time.

4. By using several fibres each sensitive to different parameters, simultaneous measurement can be achieved by one fibre using fibre coupling. Alternatively multi-parameter sensing can be achieved by different chemicals bonded to one single optical fibre.

5. High information density can be achieved since the guided light can differ with respect to wavelength, phase, decay profile, polarisation or intensity modulation. For example an optical fibre can simultaneously transmit blue

light in one direction and orange light in the opposite direction.

A Step-index multimode fibre and its main components are shown in Figure 1.1. The fibre has a central core (refractive index n_1) and is surrounded by a cladding (refractive index n_2) . The outer protective layer is referred to as the primary coating.

The optical fibre uses the concept of Total Internal Reflection (T.I.R.) for the propagation of light and this is explained in greater detail in Chapter 2. The principle behind T.I.R. relies on reflection at an interface between media of different refractive index. The core of the fibre is of a higher refractive index than the cladding. Therefore propagation is achieved by multiple reflections at the core/cladding interface.

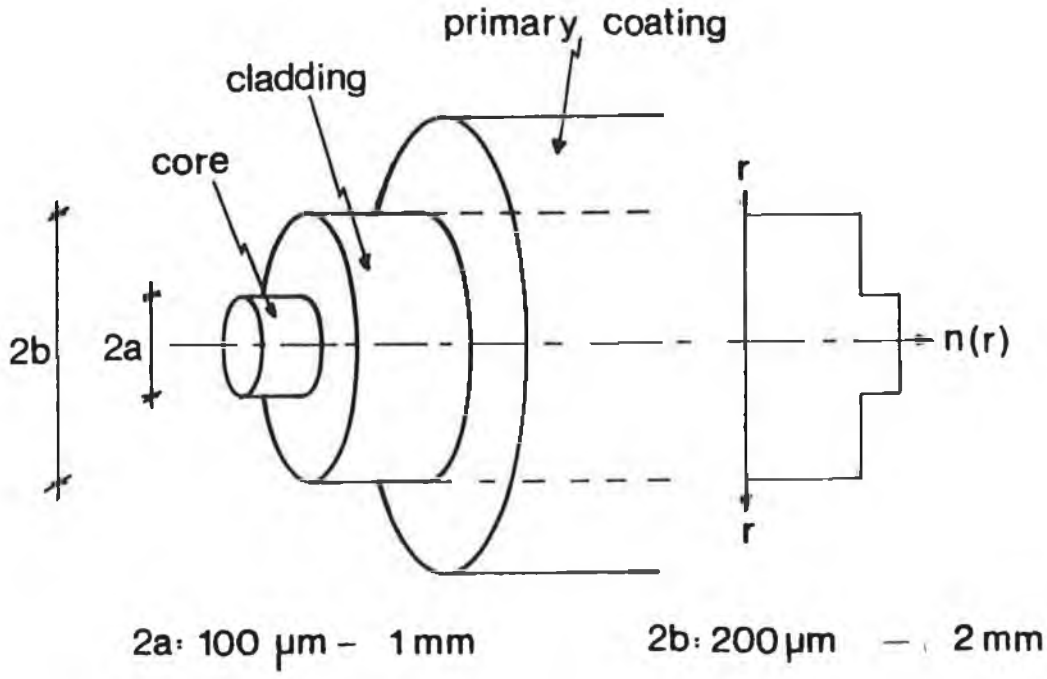

Figure 1.1 Diagram of a typical Step-index Multimode fibre with its refractive index profile.

Core diameters can range from 4 µm for single mode fibres to over 1 mm for large multimode fibres. The fibres used

in this work are multimode and have a typical diameter of 600 μm and the fibre including the primary coating is approximately 1.5mm in diameter.

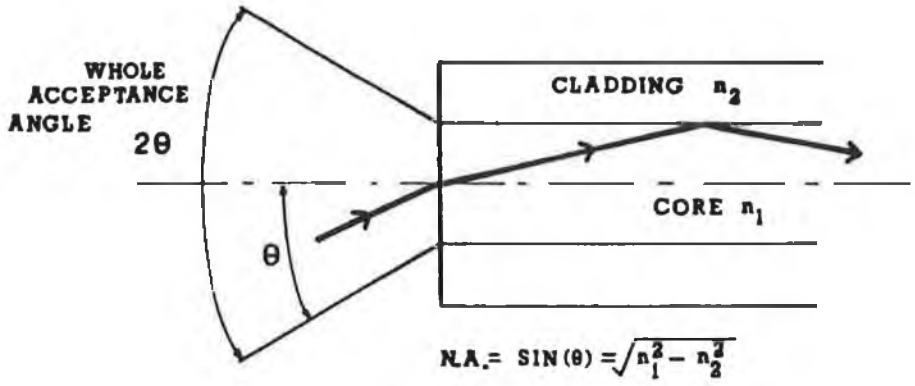

Figure 1.2 Diagram of fibre showing acceptance angle.

Two important parameters in the characterisation of an optical fibre are the Numerical Aperture (N.A.) and the V-number:

$$N.A. = \sqrt{n_1^2 - n_2^2} \quad \ldots\ldots\ldots\ldots 1.1$$

$$V\text{-number} = \frac{2\pi a N.A.}{\lambda} \quad \ldots\ldots\ldots\ldots 1.2$$

where n_1 and n_2 are the core and cladding refractive indices respectively, a represents the core radius and λ is the free space wavelength.

The refractive index of the core (n_1) and of the cladding (n_2) determine the acceptance angle θ of the fibre (see Figure 1.2). The Sine of this angle is defined as the *Numerical Aperture*(N.A.) and is given by Equation 1.1. Light must fall inside this angle to be guided within the fibre.

The Normalised Frequency Parameter, commonly called the *V-number* of a fibre is a unitless number which is important in determining which of the allowed

electromagnetic field distributions *(modes)* will be supported by a fibre. The V-number is a unique number for a given fibre.
In addition, the number of modes which a fibre can support is given by [40]:

$$\text{Number of modes} \propto \frac{V^2}{2} \quad \text{.....1.3}$$

There two approaches which can be adopted in the analysis of the propagation of light in optical fibres-the *Modal approach* and the *Ray-optic* approach.

In the modal approach, propagation of light in a multimode fibre is described using Maxwell's electromagnetic equations which are applied to a cylindrical waveguide with certain boundary conditions such as the radius r, core and cladding refractive indices, discontinuity at r = a (the core/cladding interface). When these equations are solved, they yield a finite number of solutions.
In the classical ray-optic approach the propagation of light in a multimode waveguide can be described using light rays because of the large size of the fibre with respect to the wavelength of light i.e. for a large V-number the ray-optic approach can be used.

1.2 Optical Fibre Sensors

Optical fibres have been used in sensing in many areas of measurement. The fibre can be used in an *extrinsic* fashion - where light actually leaves the fibre and before re-entering the fibre interacts with an external stimulus. For example, when two fibres are placed at 90° to one another they create a sample volume by the interaction of their respective launch cones. This method is employed in the analysis of algae (containing chlorophyll) growth in water for certain environmental sensors. One fibre guides the

excitation light and the collecting fibre gathers the resulting fluorescence from the algae. In the *intrinsic* case the fibre itself acts as the sensing medium rather than purely as a carrier of light. For example, by simply bending an optical fibre one can induce a loss in intensity caused by light leaking out into the cladding. Sensors designed to measure strain were designed using this concept.

In recent years the area of fibre optic sensing has combined with that of chemistry to yield a group of sensors that use chemicals that react with their local environment. Numerous organic, biorganic and inorganic analytes have been shown to exhibit either absorption, fluorescence or phosphorescence when irradiated.
These type of sensors can be divided into two main areas,

(1) remote fibre sensing where light is guided over a large distance both to and from the sensing region
or (2) as an *optrode* where a probe type sensor is constructed by a chemical bonded onto an optical fibre. For example, Wolfbeis et al [41] designed an optrode that is sensitive to Oxygen. The optrode consists of an Oxygen sensitive dye, (a Klesegel-adsorbed fluorescent metal-organic complex), entrapped in a gas permeable polymer matrix attached to the end of the fibre.
Both the optrode and remote fibre sensing can be utilised either in a direct way by attaching the chemical to the distal end of the fibre or in an *evanescent wave* (E.W.) configuration. In this configuration optical fibres with an unclad section can be used to detect chemical species using the attenuation of the evanescent wave which exists outside the fibre core as shown by many workers [2,3,4,5,8,9]. In addition, the evanescent field can be used to excite fluorescence from specific dye complexes located near the core surface. Evanescent wave (E.W.) excited fluorescent based devices together with the optrode concept provides the initial motivation for the

development of disposable tip sensors and the work described in this thesis.

1.3 Introduction to Fluorescence

The theory of fluorescence is well understood and well reviewed by Guilbault [25]. A molecule in its ground state may, by the absorption of a photon of sufficient energy, be raised to a higher unstable excited level (an excited singlet state). On returning to its ground state a photon is spontaneously emitted. Some energy is lost before decay by internal conversion (a rapid relaxation to the lowest vibrational level of the excited state). This results in an emission wavelength that is always longer than that of the photon used to excite the molecule to its higher energy level. This type of fluorescence is called *Stokes Fluorescence.* Each absorption to the first excited state will have a corresponding emission or fluorescence band.In addition the fluorescence peak will be at the same wavelength regardless of the excitation wavelength; the fluorescence intensity will however vary with the strength of absorption. The fluorescence intensity is related to the dye concentration by the following expression:

$$I_f = \phi\, I_o\, (1 - e^{-\varepsilon L c}) \quad \text{.....1.4}$$

where I_o is the incident radiant intensity,
ε is the molar extinction coefficient,
L is the optical path length in the sample,
c is the dye concentration,
ϕ is the fluorescence quantum efficiency.

(The factor $I_o e^{-\varepsilon L c}$ is the Beer-Lambert power absorption)

For low concentrations ($\varepsilon Lc << 1$) the fluorescent intensity is directly proportional to the dye concentration,

$$I_f = \phi\, I_o \varepsilon L c \quad \text{.....1.5}$$

Various additional factors may affect the intensity of fluorescence and are listed below:

(a) The Inner Filter effect

(b) Quenching

(c) Photodecomposition

(a) The Inner Filter Effect

The inner filter effect occurs at high concentrations of the emitting species. For low concentrations the relationship between the fluorescence intensity I_f and the concentration is described by Eqn.1.3 and is illustrated by the linear region in Figure 1.3.

At higher concentrations the curve begins to level off as the higher power terms in the expression $e^{-\varepsilon Lc}$ become more significant.

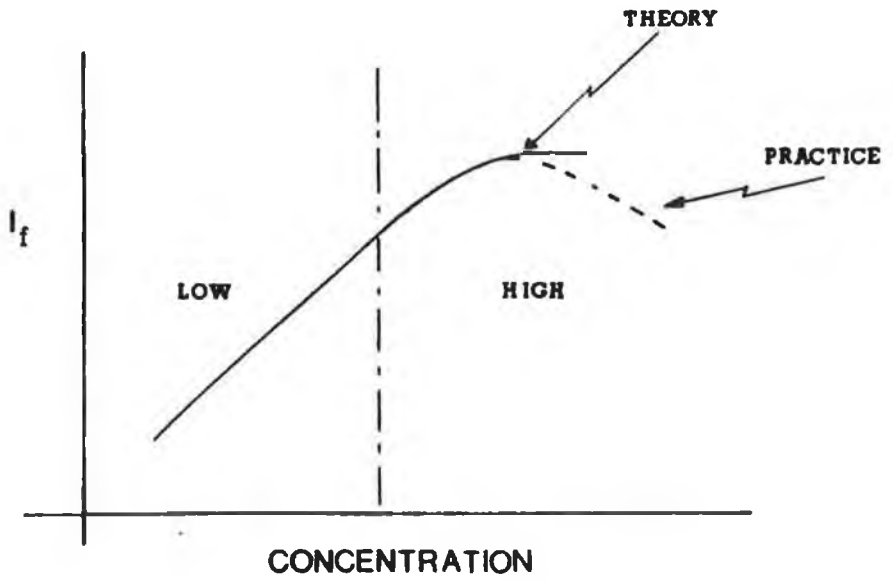

Figure 1.3 Graph of the intensity of fluorescence I_f against concentration taken from Guilbault [25].

Experimentally the Fluorescence .v. Concentration curve exhibits a maximum. The theoretical model fails to predict this even when all the significant higher power terms are included. Therefore there must be another effect taking

place. The reason for this additional curvature is that at high concentrations each layer of the sample absorbs some of the incident light so that the incident intensity is progressively reduced as it passes through the sample. This is the inner filter effect. The value of I_o which was assumed to be constant actually decreases for most regions of the sample at high concentration levels.

(b)Quenching

Quenching can be defined as the reduction of the fluorescence process by a competing deactivating action resulting from specific interactions between the absorbing species and another factor present in the system. Quenching involves the removal of energy from an excited molecule by another molecule usually as a result of a collision. For example the fluorescence intensity falls as the temperature of the sample increases. This is known as temperature quenching. The quenching of fluorescence may be used as a sensing mechanism for the presence of a particular chemical species.For example a Ruthenium complex $Ru(bpy)_3^{2+}$ is quenched in the presence of Oxygen. For high concentration levels self-quenching is a significant factor and is closely related to the inner filter effect. However, the inner filter effect contributes more to the reduction of the fluorescence mechanism.

(c)Photo-decomposition

The photo-decomposition process is a process that competes with the emission process. The most common type of photo-decomposition is bleaching. The process results in a decrease in the intensity of fluorescence and is mainly due to the photon energy being comparable with the band disassociation energy of the absorber.The absorber does not recover from the bleaching process and it is thought that the structure of the fluorescent molecule is damaged.

The amount of bleaching or the rate at which the fluorescent intensity decreases is found to increase at

higher incident intensities and is less significant at low concentrations. The combination of photo-bleaching, quenching and the inner filter effect means that the decay of the intensity of fluorescence over time is not a simple relationship.

1.4 Evanescent Wave (E.W.) Fluorescent Based Devices

Using the evanescent wave technique together with appropriate fluorescent dyes a sensor can be designed to sense such parameters as Oxygen and Carbon Dioxide. The main developments of evanescent wave based devices is derived from biological,medical and environmental applications. Andrade et al [42] described a technique for monitoring antigen-antibody reactions in a competitive immunoassay, in which a fluorescent-labelled antigen or antibody competes for binding sites on biomolecules immobilised (chemically bonded) to the fibre surface. Sutherland et al [13] used a similar evanescent wave technique to monitor antibody-antigen reactions at a solid/liquid interface. They were able to detect the bonding reaction in real-time and hence providing vital information for biological applications.

The motivation for this work is derived from the ability of fluorescent dyes, that are immobilised or entrapped on an optical fibre surface, to:

1. be excited evanescently, and
2. be sensitive to their local environment.

In addition, evanescently excited fluorescent dyes can be carefully immobilised onto an optical fibre yielding a specific sensing region. This sensing region can be either located at the end of a long fibre optic cable to give remote E.W. fluorescent sensing or immobilised on a short length of fibre to provide a disposable tip sensor or a unique sensing element to be used in multi-sensor arrangement.

In this work an optical system was designed for the E.W. excitation and collection of evanescently excited fluorescence (Chapter 3). Two methods of attaching dyes were investigated:

(a) chemical immobilisation (Chapter 5), and

(b) entrapment in a porous glass coating formed by the Sol-gel technique.(Chapter 5)

For each technique, the dye spectra were examined for spectral consistency, spectral shape, intensity of fluorescence, quality of coatings and the ease at which the coating could be achieved.

The novel technique of entrapping fluorescent dyes into a porous glass coating around the core of optical fibres (i.e. the Sol-gel) method proved to yield more consistent coatings. This technique is described in Chapter 4.

Both methods were tested, using a pH sensitive dye, for their performances in aqueous environments in which the pH could be varied. These results are discussed in Chapter 5.

CHAPTER 2
EVANESCENT WAVE EXCITATION OF FLUORESCENCE

2.1 The Evanescent Wave

At the interface of two media of refractive indices n_1 and n_2 with $n_1 > n_2$ *total internal reflection* occurs when the incident angle θ in the denser medium is greater than the critical angle θ_c given by $\mathrm{Sin}^{-1}(n_2/n_1)$ as shown in Figure 2.1.

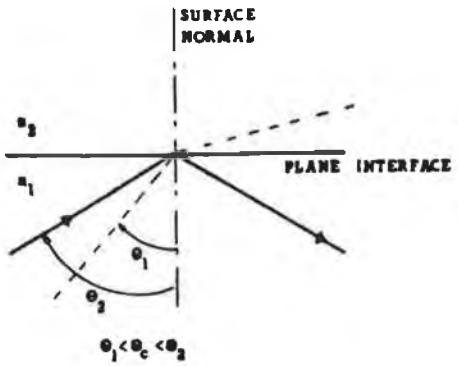

Figure 2.1 Diagram of two rays incident on a plane interface.

In the dense medium, the superposition of the incoming and the reflected beam will generate a standing wave and in the rare medium a non-propagating, exponentially decreasing field with distance into the medium is formed. This is shown in Figure 2.2. A theoretical development of how the evanescent wave is formed is given in Appendix A1.

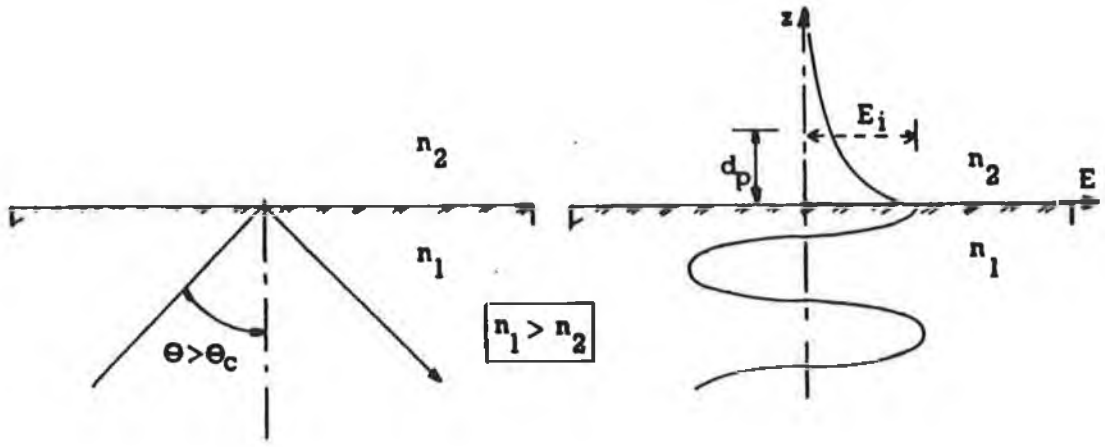

Figure 2.2 Diagram of the evanescent wave generated at an interface.

This non-propagating E-field is given by

$$E_z = E_i \, e^{-z/d_p} \quad \ldots\ldots\ldots\ldots 2.1$$

where E_i is the electric field amplitude at the interface,
z is the distance into the rare medium perpendicular to the interface,
and d_p is called the penetration depth which is given by

$$d_p = \frac{\lambda}{2\pi n_1 \left(\sin^2\theta - (n_2/n_1)^2 \right)^{1/2}} \quad \ldots\ldots\ldots 2.2$$

where λ is the free space wavelength,
n_1 is the refractive index of the dense medium,
n_2 is the refractive index of the rare medium,
θ is the angle of incidence with respect to the normal to the interface.

Values for the penetration depth can be obtained by considering a glass/water interface where $n_1 = 1.458$ and $n_2 = 1.333$. By choosing two values for θ , $\theta = 75^\circ$,-a typical value for θ and $\theta = 67^\circ$- a value very close to θ_c, the penetration depths are found to be 0.35λ and 1.03λ. This

clearly indicates the importance of working at angles close to the critical angle.

Since intensity is proportional to the amplitude squared the optical power in lower index medium can be written as

$$I_z = I_i \, e^{-2z/d_p} \quad \ldots\ldots\ldots\ldots\ldots 2.3$$

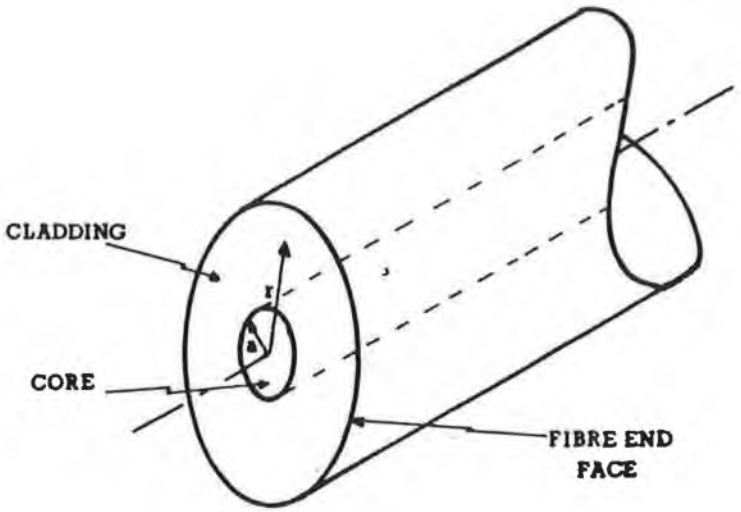

Figure 2.3 Diagram of fibre optic launch face.

In the case of optical fibres light is guided by T.I.R. and thus the evanescent wave amplitude in the cladding near the core/cladding interface may be written as

$$E = E_i e^{-(r-a)/d_p} \quad \ldots\ldots\ldots\ldots 2.4$$

where E_i is the amplitude at the interface with r and a as illustrated in Figure 2.3.

The evanescent intensity can therefore be written as

$$I(r) = I_i e^{-2(r-a)/d_p} \quad \ldots\ldots\ldots\ldots 2.5$$

where I_i refers to the intensity of the light at the core/cladding interface.

A complete treatment of light propagation in optical fibres requires the application of Maxwells equations and

the appropriate boundary conditions in cylindrical coordinates. When this is done the solution is a standing wave parallel to the interface and an evanescent component exponentially decreasing with distance into the rare medium (see Figure 2.4)

2.2 Evanescent Wave Interactions

In Figure 2.4 a schematic diagram of the evanescent wave penetrating into the fibre cladding and the standing wave pattern formed by the superposition of the incoming and reflected light is shown.[17]

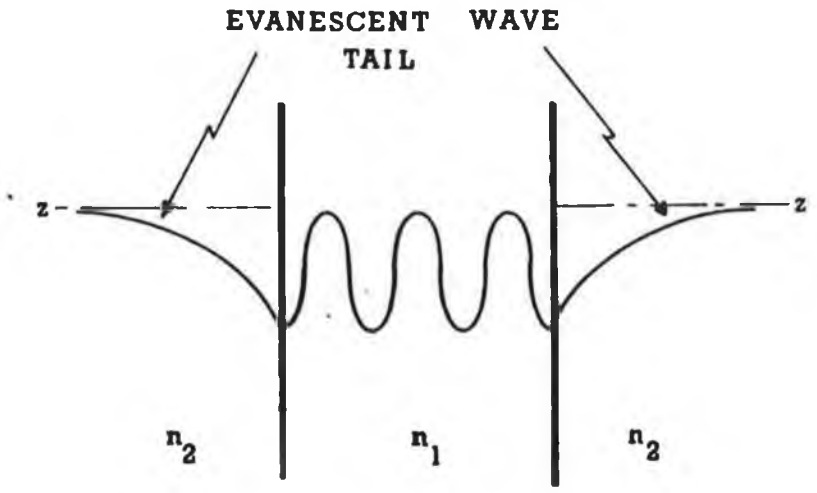

Figure 2.4 Waveguide showing standing wave pattern in the core and evanescent wave in the cladding.

In the case of a lossless low index medium (with a refractive index with a negligible imaginary component) there is a zero net flux of light across the interface. In this case the Fresnel reflection coefficients $R_{\perp}$ and $R_{\parallel}$ have a value of unity as shown in Figure 2.5.

When the lower index is lossy the refractive index can be written as n - ik where n is real component of the refractive index and k is related to the absorption coefficient α by $\alpha = 4\pi k/\lambda$.

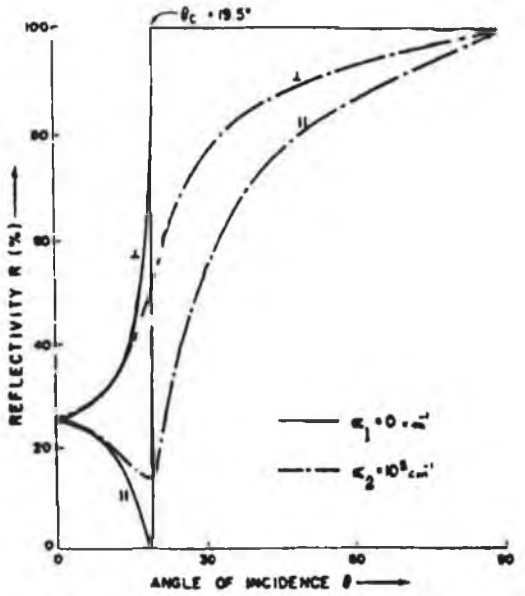

Figure 2.5 The Reflectivity R against the angle of incidence θ with $n_{21} = 0.33$ for two cases [17];
case 1, for a non-absorber $\alpha = 0$ cm^{-1}
case 2, for an absorber $\alpha = 10^5$ cm^{-1}

The effect of the lower index medium becoming an absorber means that the Fresnel power reflection coefficients become slightly less than unity for the two orthogonal polarisations. This case is illustrated in Figure 2.5 as a strong absorber.
This results in a net power flux across the interface between the core and cladding.

In the case of optical fibres, losses at each reflection give rise to an attenuation in the guided power given by,

$$P(y) = P(o)\ e^{-\gamma y} \quad \ldots\ldots\ldots\ldots\ldots\ldots 2.7$$

where y is the direction along the longitudinal axis of the fibre and γ is the evanescent absorption coefficient. The evanescent absorption coefficient depends linearly on the concentration of the species giving rise to the absorption [44].

This is true only if the latter obeys the Beer-Lambert law of absorption.The absorption coefficient α is related to γ by the relationship,

$$\gamma = r\,\alpha$$

where r is the fraction of power outside the fibre core. This fraction may be expressed as $r = 4\sqrt{2}/3V$ in the case of multimode fibres where $n_1 \simeq n_2$ described by Gloge [39].

If the absorber is a fluorescent molecule, fluorescent emission will take place when the evanescent wave interacts with it. The fluorescence is emitted in all directions within the cladding, although not in an isotropic fashion as is explained later.

From a ray-optics approach it is not obvious that optical energy originating in the cladding will be guided by the core. A light ray which enters the core from the lower index cladding travels at an angle less than the critical angle for T.I.R.. Thus every such ray is expected to leak out after a few reflections. Experimental measurements indicate this not to be the case and E.W. excited fluorescence may re-enter the core and be guided by the fibre. Ray optics is insufficient to treat this "coupling" effect.

In order to obtain knowledge of how the fluorescent light is coupled back into the fibre core one must approach the problem from a wave optics point of view. Using this approach the evanescent wave in the cladding interacts with an absorbing center (the fluorescent dye molecule) to produce fluorescence which is "coupled" back into the fibre core. This can only occur if the emitted fluorescence is itself evanescent in nature and forms an evanescent wave with a corresponding guided standing wave in the core. This is the Principle of Reciprocity which will be discussed in more detail in the next section.

2.3 Properties of E.W. excited fluorescence

In this section an expression for the E.W. excitation of fluorescence captured by an optical fibre is developed.

It was shown in Section 1.3 that at low concentrations the intensity of fluorescence is directly proportional to the product of the concentration of the fluor and the intensity of the excitation light I_0.
In order to obtain the total fluorescent signal captured by an optical fibre, one must integrate over the entire interaction volume formed by the evanescent wave.

In our analysis to follow, the classical ray-optics approach is used and hence all angles from the critical angle θ_c to $\pi/2$ are allowed [16]. For the case of an optical fibre (step-index multimode) the total fluorescent intensity is therefore given by

$$I_F \propto \phi\varepsilon I_0 \int_{\theta=\theta_c}^{\pi/2} \int_{r=a}^{\infty} \int_{y=0}^{L} c(r)\, e^{-2(r-a)/d_p}\, 2\pi r\, dy dr d\theta \quad \ldots\ldots 2.8$$

where y is the distance along the fibre,

$c(r)$ the fluor concentration in the cladding region,

d_p the penetration depth of the evanescent wave which is a function of θ,

ϕ the quantum efficiency of the fluorescent material,

ε the molar absorptivity of the fluorescent material

and I_0 the excitation intensity.

When the dye is in solution about the fibre the concentration c is no longer dependent on position r and integrating over the length L of the interaction region, the fluorescent intensity is then given by

$$I_F \propto \phi\varepsilon c\, L\, I_0 \int_{\theta_c}^{\pi/2} \int_{r=a}^{r=\infty} e^{-2(r-a)/d_p}\, 2\pi r\, dr d\theta \quad \ldots\ldots\ldots 2.9$$

i.e. the intensity is directly proportional to the dye concentration,the sensing length and the excitation intensity.

The Principle of Reciprocity is vital in the understanding of how fluorescently excited light originating in the cladding can be coupled into the core. Carniglia et al [11] investigated the excitation of fluorescent molecules located in a rare medium using E.W. excitation.They described the absorption of evanescent field and the reciprocal effect, namely the emission of an evanescent field by excited molecules located in the rare medium.They observed that the angular dependence for the absorption and the emission processes were identical. Their work verified the principle of reciprocity and indicates how evanescently excited fluorescence originating in the rare medium can be coupled back into a dense medium. However, it is not obvious how light originating in the cladding may be guided by the core. Lieberman et al [14] suggested that light emitted by a source in the cladding can have a spatial dependence that resembles the decaying exponential associated with a guided mode in the core. This spatial dependence results in a bound mode which exhibits the wavelength nature of the source located in the cladding. Thus it is thought that the evanescent fields of the guided modes provide a path for this "coupling".

More recently Marcuse [15], using an external light source around the cladding of a step-index multimode fibre, addressed the efficiency of light injection into the core of the fibre from fluorescent sources located within the cladding region. He reasoned that light sources in the cladding could interact with the evanescent tails of the guided modes within the core thereby transferring some power into core. He estimated that approximately 0.01% of the power in the cladding could enter the core by this mechanism.

Lieberman at al [14], using fused silica fibres with a

Polydimethyl Siloxane cladding in which an Oxygen sensitive dye was located, measured coupling efficiencies of the order of 1×10^{-4}, in close agreement with the work of Marcuse.

In attempting to derive an expression for the detected E.W. excited fluorescence one must consider two additional parameters:

1. The ratio of the E.W. excitation power (in the cladding) to that of the guided excitation power (in the core) i.e. the excitation coupling efficiency η_1.

2. The ratio of the fluorescent power in the core to the fluorescent power in the cladding i.e. the emission coupling efficiency η_2.

η_1 is clearly related to the penetration depth of the evanescent field and η_2 is the coupling efficiency of the E.W. excited fluorescent light coupled from the cladding into the core.

Thus, in the case of E.W. excited fluorescence of a fluorescent dye located near a fibre core surface, the detectable fluorescent intensity is given by

$$I_f \propto I_o \eta \phi \varepsilon L c \quad \ldots\ldots\ldots\ldots\ldots\ldots 2.10$$

where $\eta = \eta_1 x \eta_2$

Love and Button [16] developed an expression for the fluorescence intensity coupled into a fibre sensor consisting of an unclad multimode step-index fibre located in a dilute dye solution. They found that the fluorescent intensity scaled both experimentally and theoretically as

(a) the sensing length (L),
(b) the intensity of the excitation source, I_0
(c) $Sin^8\theta_{max}$ where θ_{max} is the maximum external angle of the launched light cone,
(d) $(n_1^2 - n_2^2)^{-2}$ where n_1 and n_2 are the core and sensing medium refractive indices respectively.

The high sensitivity to Sin θ_{max} in (c) above indicates the very high dependence of the excitation efficiency on the proximity to the critical angle. At angles near the critical angle the penetration depth becomes very large and hence increases the evanescent excitation volume around the core of the fibre. This provides motivation to work with launch angles close to the critical angle.[17, p.31]

2.4 Conclusions

Evanescently-excited fluorescence which is coupled back into an optical fibre has the following properties:

(1) The detected intensity depends strongly on the evanescent penetration depth. By operating at angles close to the critical angle one can achieve a large sensing volume.
(2) The detected intensity increases linearly with the interaction length.
(3) The detected intensity is inversely dependent on the fourth power of the local numerical aperture $(n_1^2-n_2^2)^{1/2}$ in the sensing region.
(4) The detected intensity depends linearly on the concentration of absorber.

CHAPTER 3

THE EXPERIMENTAL SYSTEM

3.1 Introduction

In this work it was necessary to record the spectra of evanescent wave (E.W.) excited fluorescence from optical fibres which had fluorescent dyes immobilised or entrapped on the surface of their cores. A system was designed taking into account the theory of E.W. excitited fluorescence outlined in Chapter 2 and also some additional design considerations such as:

1. The system must separate the excitation radiation from the returning fluorescent light.
2. The system must collect the returning fluorescent light as efficiently as possible.
3. The emission spectra of the fluorescent dyes must be taken into account.

3.2.1 The Optical System

A schematic diagram of the experimental system is shown in Figure 3.1. The optical system consists of a laser, two lenses, two microscope objectives, a dichroic filter, a micropositioner and a scanning monochromator.

The fluorescent dyes that were used in this work absorb significantly at 488nm and have emission spectra in the range 500nm to 600 nm. Therefore an Ar-ion laser was used as an excitation source (with the 488nm laser line selected). To separate the excitation light from the returning fluorescent light a dichroic filter that reflects 488nm laser light and has a transmission window in the region of 500nm to 600nm was used. Its transmission spectrum is shown in Appendix A2.

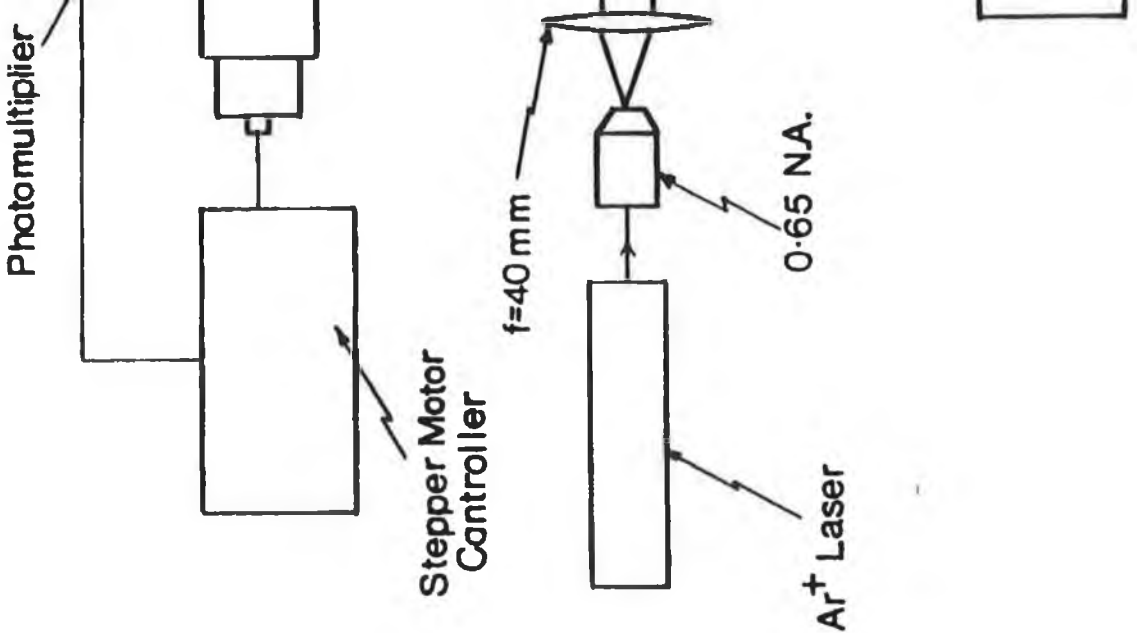

Figure 3.1 A schematic diagram of the experimental apparatus

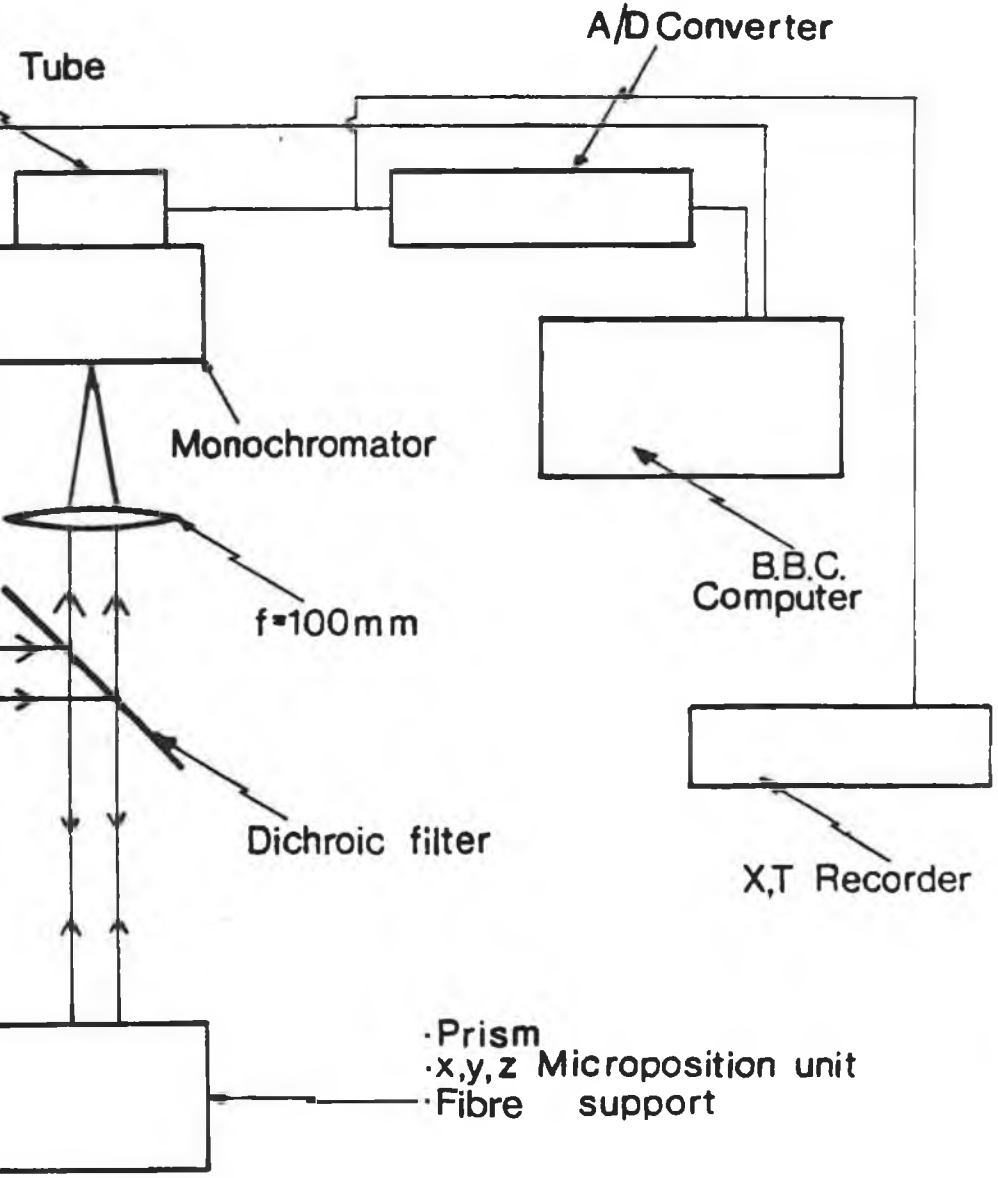
A/D Converter
Tube
Monochromator
B.B.C.
Computer
f=100mm
Dichroic filter
X,T Recorder
·Prism
·x,y,z Microposition unit
·Fibre support

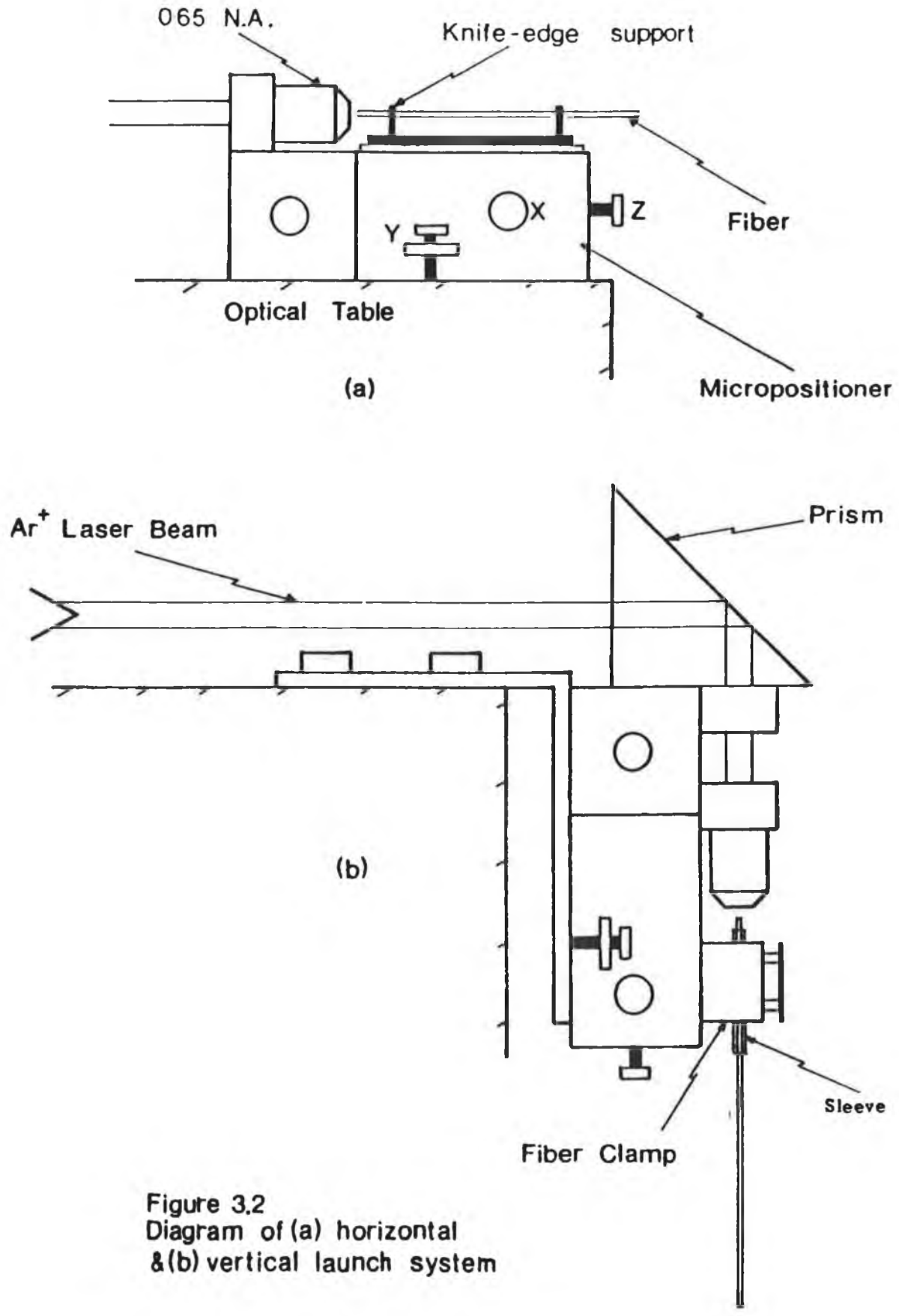

Figure 3.2
Diagram of (a) horizontal
&(b) vertical launch system

The general system operates as follows: light from an Argon ion laser is collimated by a 40 mm focal length convex lens (of diameter 25 mm). The collimated light travelling horizontally is incident on a dichroic filter placed at 45° to the direction of propagation.The collimated laser light is reflected by the dichroic filter and is then incident on a horizontal (Figure 3.2(a)) or vertical (Figure 3.2(b)) launch system. Laser light is then launched into a fibre where it evanescently excites fluorescence. The fibre is held in position by a fibre clamp located on the top surface of the micropositioner. The returning longer wavelength fluorescent light is coupled along the same path and is then transmitted by the dichroic filter.It is then focused down by a 100 mm focal length convex lens into a scanning monochromator. The light is then detected by a Hamamatsu R1546 photomultiplier tube at the rear of the monochromator. The analog output signal of the photomultiplier is digitised using a 12 bit A/D and fed to a micro-computer. Thus the emission spectrum of the fluorescent material can be stored as a intensity versus wavelength file on disc. The software used for the operation of the system is included in the Appendix A3.

3.2.2 System Efficiency Considerations

From the theoretical considerations outlined in Chapter 2, the launch system (for launching light into the fibre) must take into account that for angles close to the critical angle the sensing volume is large yielding a large E.W. excited fluorescent signal. Initial work was carried out using a fibre, whose primary coating and cladding were removed, in a Rhodamine6G/water solution. For these conditions the critical angle at the glass/water interface is $\simeq 66^{\circ}$. Working in reverse one can calculate that the launch angle required at the launch face (air/glass interface) has a value of 36°. By using a microscope objective of 0.65 N.A. with $\theta = 40.5^{\circ}$ a

range of interface angles of 90° to 64°can be achieved. Secondly, to obtain efficient collection E.W. excited fluorescence, the f-number of the monochromator was matched by including a 100mm focal length lens of diameter 25mm which was placed in line with the entrance slit of the monochromator.

The monochromator is based upon the Fastie-Ebert mount design shown in Figure 3.3.

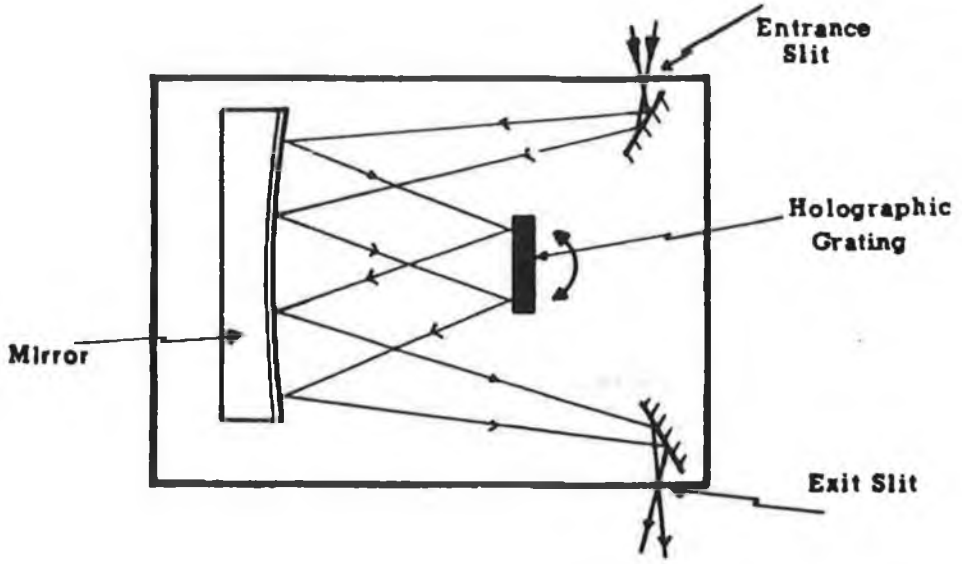

Figure 3.3 Internal optical configuration of the monochromator.

The monochromator has an effective focal length of 74mm and an f-number of 3.8.

A table of the resolution/ slit-width relationship is shown in Table 3.1.

Slit Width (μm)	Resolution (nm)
200	0.9
300	1.8
600	3.6

Table 3.1 Showing the monochromator resolution dependence on slit width.

During initial experiments the fluorescent signal was found to be low, hence to achieve a large signal to noise ratio a slit with of 600μm was chosen with a corresponding resolution of 3.6 nm.

3.2.3 The Source

The source used in this system was a Cathodeon Model C840 air-cooled Argon ion laser. Its rated output power is 100 mW in multi-line operational mode. There are a range of wavelengths which this laser can produce and these are listed below:

λ (nm)	POWER(mW) at 8.8A
457.9	7
476.5	10
488.0	32
496.5	12
501.7	3
514.5	42

Table 3.2 Showing the laser power at each laser line at a tube current of 8.8A.

For all the experiments carried out in this project the 488 nm laser line was selected. The plasma tube (containing Argon) made from Beryllium oxide constrains the discharge to a narrow beam by the nature of its design and is shown in Figure 3.4.

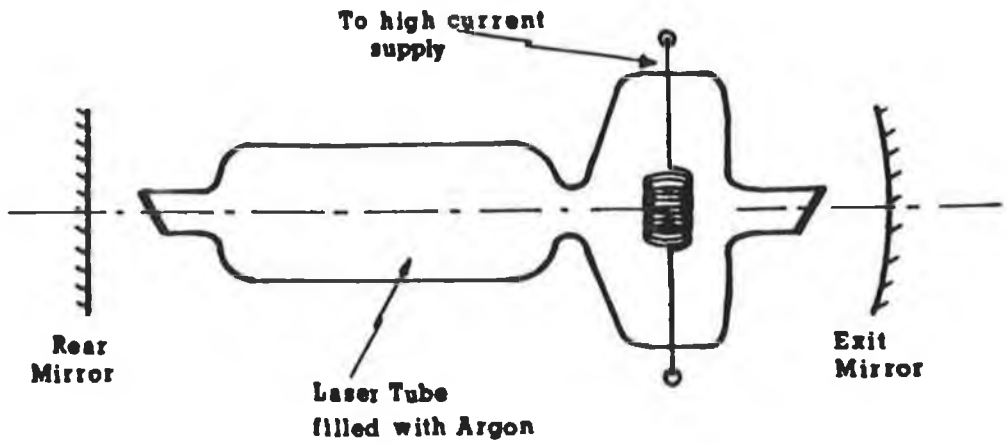

Figure 3.4 Diagram of laser cavity.

The two optical mirrors within the laser are plane and spherical concave respectively to form a Fabry-Perot cavity. Adjustment of the rear mirror will cause angular displacement of the beam while adjustment of the exit mirror will result in lateral displacement of the beam. The flash tube current is monitored internally and maintains a constant output power when used in the *lightmode* operational mode.

3.2.4 The Detector

The detector was a Hamamatsu R1546 photomultiplier tube.

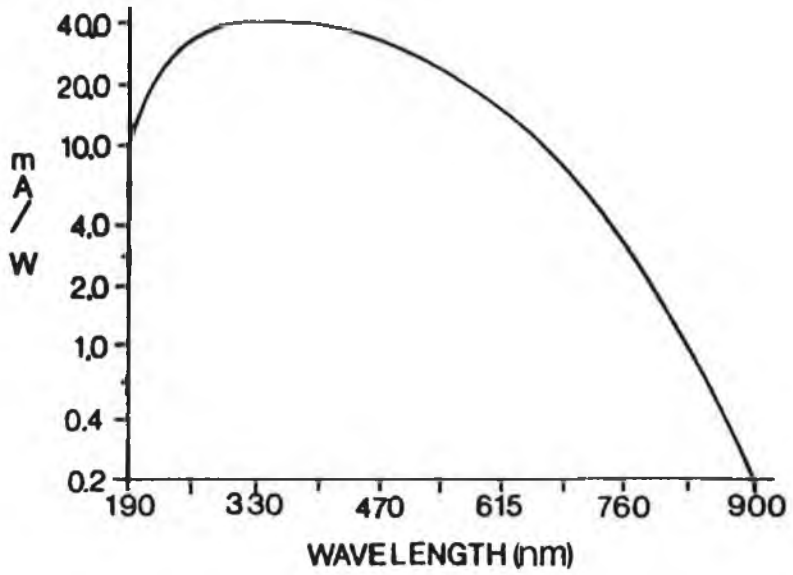

Figure 3.5 Spectral response of the photomultiplier tube.

It consists of a 12 mm multi-alkali photomultiplier tube integrated with an adjustable high voltage power supply (0 to -1000 Volts dc). An operational amplifier with an adjustable gain is included with the unit.There is an adjustable dc offset to allow for ambient light levels.The photo-cathode is of a multi-alkali type containing Sodium, Potassium, Antimony and Cesium and its window material is made of U.V.glass. The spectral response of the detector is shown in Figure 3.5. The detector has a window from 185 nm to 850 nm and peaks at 530 nm and its response time is of the order of 14 ns. The photomultiplier is mounted directly onto the exit slit of the monochromator.

The optical system and the detector are mounted on a vibration free optical bench as shown in Figure 3.6.

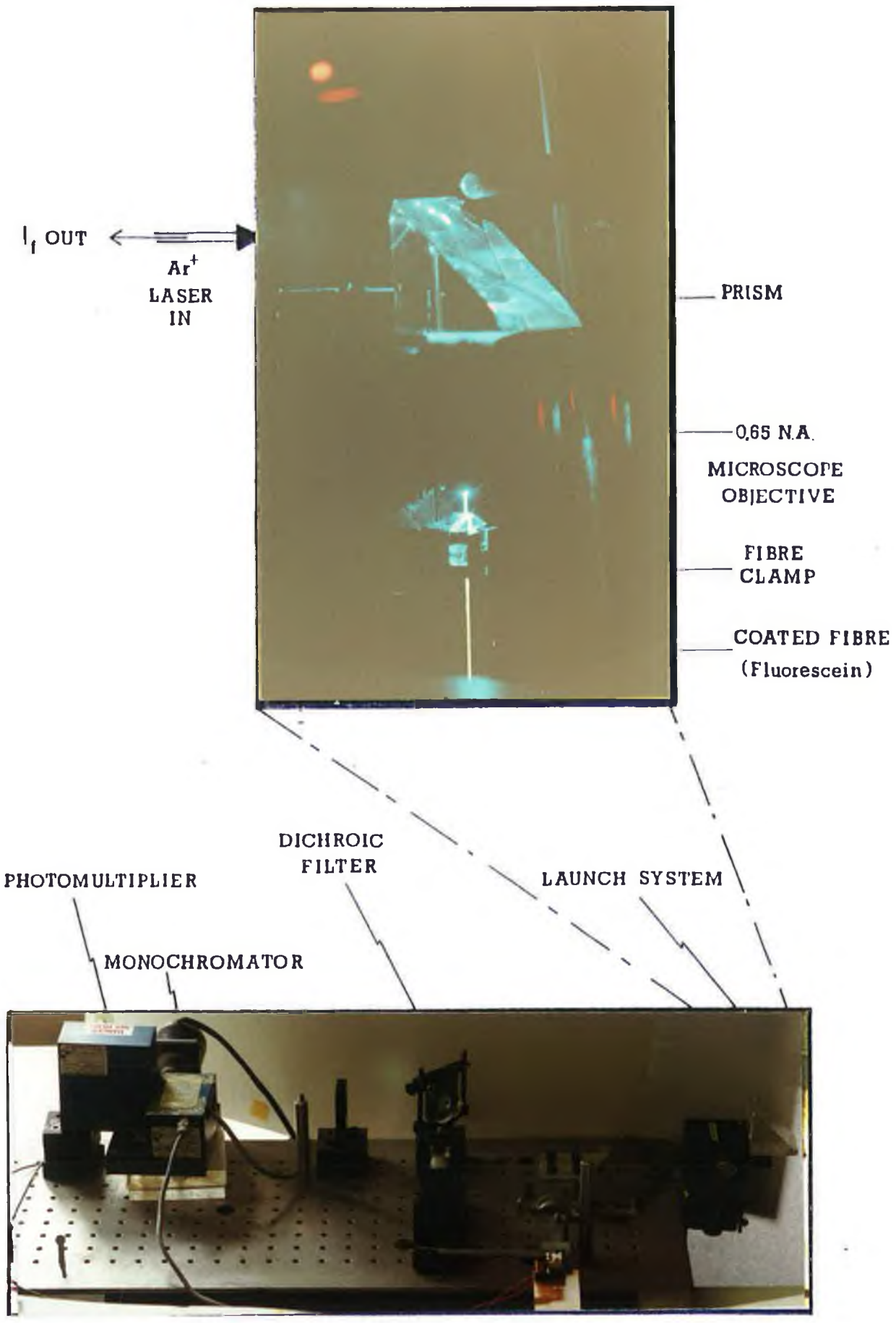

FIGURE 3.6 DIAGRAM OF THE OPTICAL SYSTEM

3.3 Preparation of Optical Fibres for fluorescence sensing

Two approaches were adopted in this work:

1. Where the sensor region is an unclad section at the far end of a long (≃ 5m) length of fibre and,

2. where the actual sensors consisted of short lengths (≃ 90mm) of fibre enabling easy preparation in terms of experimental work and allowing the eventual conversion to a disposable tip type sensor .

The type of fibre used in this project is a Plastic Clad Silica (P.C.S.) fibre of core diameter 600μm. As standard fibre optic cleaving tools are not able to accommodate this relatively large diameter fibre the fibres must be broken and then polished at each end. The fibre was first cut into 9cm long pieces and approximately 30 of these *rods* are then put into a chuck to facilitate polishing of the ends. Three of these chucks are placed into a chuck holder ready for polishing (see Figure 3.7). The rods are left standing proud of the polishing chuck approximately 4 mm because it was observed that surface damage occurred during cutting over a length of 2 mm. The chuck holder containing all of these rods is then placed on a polishing rig as shown in Figure 3.8.

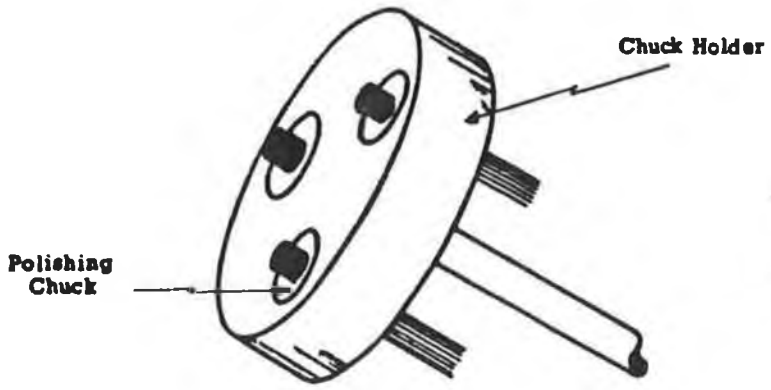

Figure 3.7 Diagram of fibre optic chuck holder.

The rig itself has a large polishing plate which rotates about a centre point. A cam linkage system links a mechanical arm which sweeps across the radius of the polishing plate. The function of this arm is to induce a spinning action into the chuck holder thereby enhancing the quality of the finished polished fibre.
Various grades of polishing fluids are supplied with the polisher. There are 9 μm, 3 μm, 0.125 μm grits available. The fluid used for the polishing of the rods in this project is a suspension of 9 μm Al_2O_3 in water.

Figure 3.8 Picture of the Polishing Rig.

The grinding action of this fluid combined with the rotation of the polishing plate and the chuck holder for a duration of 3 hours polishes the end faces of the rods. The rods are then taken out of the chucks, inverted and the above is repeated for the other end face. The result is an 8cm long P.C.S.600 rod with two polished end faces.

Each rod in turn is then cleaned first by water to remove most of the Aluminium Oxide and then with Ethanol to remove any remaining grit.The rods are then closely examined individually for the polishing quality. Any non-standard rods- for example one with a cracked end face - are rejected. The primary (protective) coating is then removed using a sharp blade to expose the fibre cladding material. The cladding material is removed by etching with a commercially available (Lumer) chemical solvent based on a Methylene Chloride, Sulphuric acid mixture. The rods are left in contact with the etchant for 12 minutes and are then washed in water. The rods are quickly placed in an ethanol bath and each rod is then cleaned with an ethanol soaked tissue. The rods are then stored in a bath of ethanol and are again inspected for any defects. The result is a batch of pure silica rods ready for dye immobilisation or dye entrapment.

3.4 Data Processing

3.4.1 The System Response

An optical system will impose its own characteristic spectral response on recorded spectra due to its component parts. The responses of the dichroic filter, monochromator and photomultiplier tube are the main contributors to the spectral response of the optical system used in this project. To acquire a *true* spectrum of a dye, for example, one must first produce an overall system response and then deconvolute this from spectra taken. If the system response is described by $SR(\lambda)$ and the actual spectra taken by $S(\lambda)$, the spectra taken can then be represented by equation 3.1,

$$S(\lambda) = L(\lambda) * SR(\lambda) \quad \ldots\ldots\ldots\ldots 3.1$$

Equation 3.1 represents the spectra taken as a convolution of a dyes spectral response $L(\lambda)$ for example and the system response $SR(\lambda)$. If a known response is used $L(\lambda)$, then the system response can be generated by the deconvolution of $L(\lambda)$ from $S(\lambda)$ as shown in equation 3.2 .

$$SR(\lambda) = S(\lambda) * 1/\ L(\lambda) \quad \ldots\ldots\ldots 3.2$$

In order to determine the system response a standard Tungsten-Halogen lamp whose spectral response was known was used. A program was developed to model the spectral response of the lamp $L(\lambda)$ and then using equation 3.2 the program generated the system response. A graph of the system response is shown in Figure 3.9. The system response curve has a peak wavelength of 554 nm and a small peak occurring at $\simeq$ 570nm due to the shape of the dichroic transmission curve.

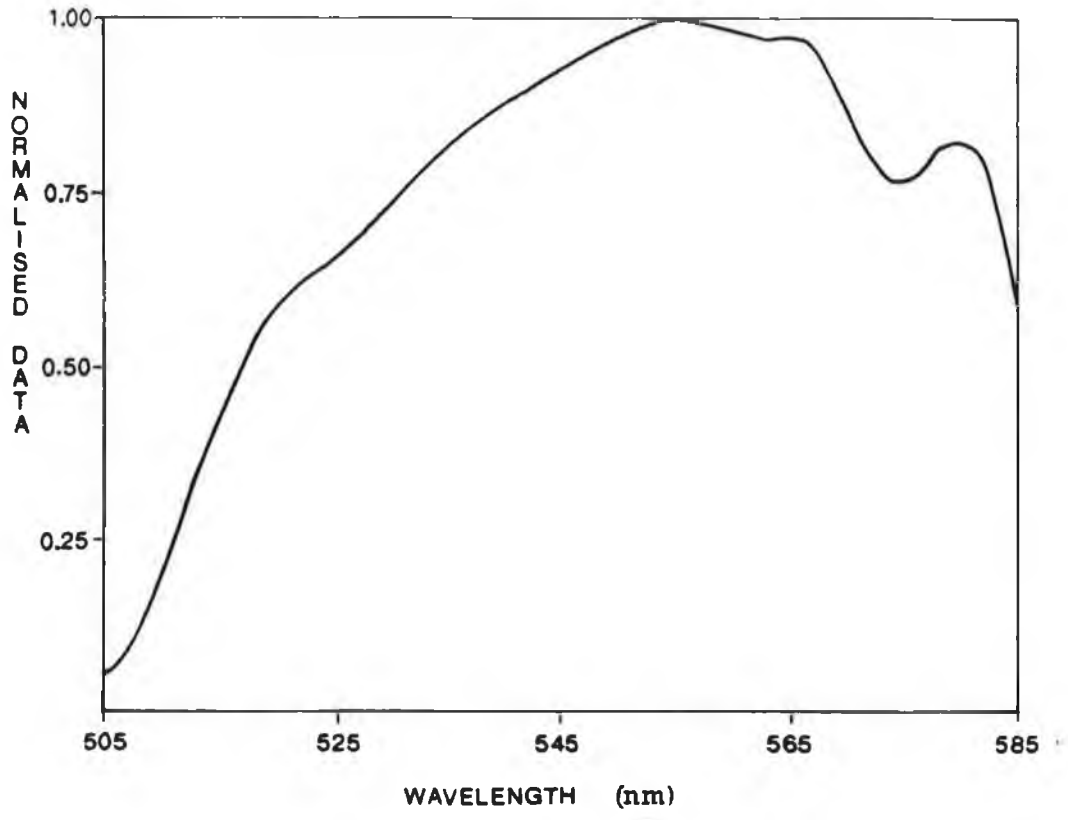

Figure 3.9 System response curve.

3.4.2 The Data Processing Procedure

For data aquisition purposes, a program previously written in this laboratory was used and is listed in Appendix A3.The data is taken via the 15 MHz bus on the micro-computer where it is sampled by the software. The main feature of the program is that it samples 500 data values at each wavelength during a scan. The average data value is then calculated and is stored on disc for each wavelength. The scan range is typically 80 nm starting at 505 nm and is incremented in 1 nm steps. This range corresponds to the transmission window of the dichroic filter.

The stored data file is searched for a minimum data value which corresponds to the ambient light level present during a scan. This data value is then subtracted off each of the values in the data resulting in an offset data file. This offset data is then divided by the system response resulting in a true spectrum of the immobilised

or entrapped dye. This approach is valid only when the recorded spectrum is known to have a full width completely contained within the dichroic filter transmission window.

CHAPTER 4

SOL-GEL COATING OF FIBRES

4.1 Introduction

In this work a method of attaching fluorescent dye molecules onto the surface of an optical fibre was required. There were two conditions which needed to be met by the technique:

1. The technique is required to attach the dye as close to the fibre core surface as possible to attain maximum absorption of the evanescent excitation field, and

2.The process should not inhibit the fluorescence of the species.

The two methods employed were: chemical immobilisation and dye entrapment using the Sol-gel technique. In the immobilisation technique, (completed by Dr.P.Greer and Mr.P.Eustace at the R.T.C.Dundalk) a fluoresecent indicator was bound to the surface of an optical fibre using various linking chemical complexes listed in Table 5.1. These linking complexes are required to make the surface of the fibre 'active' so that the dye will bind to this layer. These techniques are described in greater detail in the results section in Chapter 5. They were not, however, found to be successful.

In the Sol-gel technique, a novel approach to entrap fluorescent dye molecules in a porous glass coating around a fibre is utilised to achieve a sensing layer which can be activated by the evanescent wave. The Sol-gel is in essence a type of glass with an open structure which results in a porous material less dense than normal glass. A glass can be defined as a material which is an inorganic product of fusion (heating/firing) which has cooled to a solid state without crystallisation. Ebelman [32], who synthesised ethyl orthosilicate for the first time in

1846, observed that on standing at room temperature, it was slowly converted into a glassy gel due to slow hydrolysis by atmospheric moisture. $Si(OEt)_4$ can therefore be regarded as the first 'precursor' for glassy materials. The innovation of mixing suitable precursors in solution for making glasses was pursued much later in the 1940's. This development, called the Solution-Sol-Gel, method has developed into the modern Sol-gel method of glass formation. The basic method of forming a Sol-gel is in three stages; the first stage is the mixing of a solution of suitable precursors i.e. metal derivatives which finally yield oxides. The second stage is the formation of a unique sol and causing it to gel; this allows chemical homogeneity to occur and is the key step in the process. The final step is the shaping of the gel into., for example bulk materials, hollow spheres, fibres, surface coatings before firing. The temperature of the heating process and the time the process lasts determine the density of the Sol-gel. Specific details are given below.
To explain more clearly what Sol-gels are a specific type of Sol-gel called an Aerogel is introduced. As its name suggests an Aerogel is made up mainly of air inside pores of a highly structured matrix made of Silica. Its structure is shown in Figure 4.1.

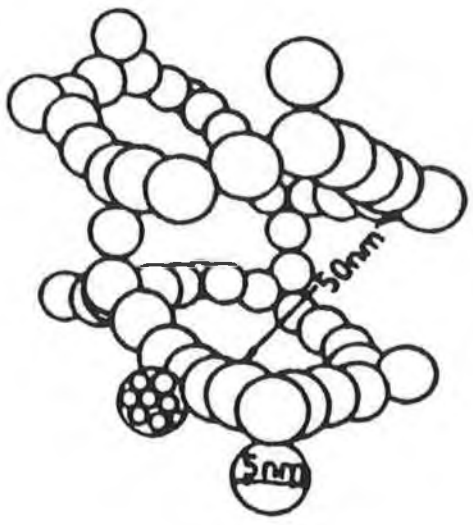

Figure 4.1 Diagram of an Aerogel structure.

The structure of the matrix is such that all of the pores are interlinked with each other yielding a completely continuous pore structure. For an Aerogel structure as shown in Figure 4.1, the particles that make up the matrix are typically less than 5 nm in diameter and the pore size is typically less than 50 nm at its widest point.

For the case of the Sol-gel materials used in this project the structure is more dense by virtue of its heat treatment. For this reason its pore size and particle size tend to be smaller. Its formation and structure will be discussed in section 4.2 of this chapter.

One of the advantages of Sol-gel technology is that the Sol-gel can be moulded into any shape. In addition the Sol-gel can be doped with various metals and can be used as an anti-reflection coating on any shaped surface. The principle of coating a curved surface is employed in this project. The Sol-gel containing a fluorescent dye is coated onto a core of an optical fibre forming a waveguide in which the evanescent wave can interact with the Sol-gel and the dopant in its pores.

This novel approach is particularly attractive for fibre optic sensor work for a number of reasons:

(1) the $Si(OEt)_4$ binds well to the fused silica core,

(2) the high specific area of the pore structure yields many dye sites which increases the sensitivity of the sensor,

(3) the continuous open-pore structure allows the diffusion of gases and liquids into the evanescent sensing region.

4.2 Formation of the Sol-gel

A Sol-gel can be thought as a state of matter intermediate between a solid and a liquid. Some biological gels are known to exist for example, the vitreous humour that fills the interior of the eye, the material of the cornea and the synovial fluid that lubricates the joints of the skeleton, where the gel network is made up of polymers derived from animal protein. Man-made gels are used as intermediates in the manufacturing of rubber, plastics and membranes.[29]

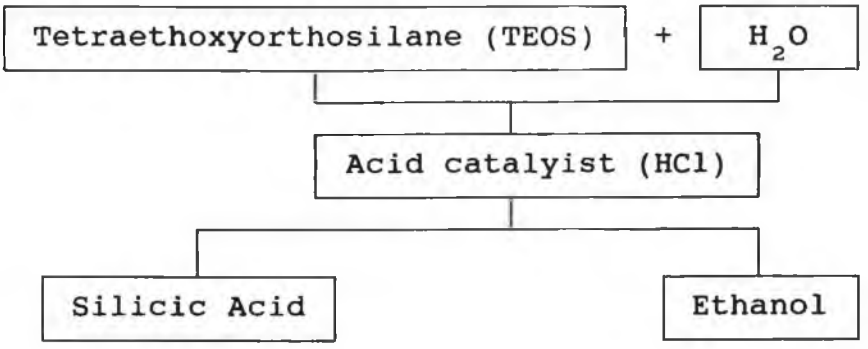

Figure 4.2 The basic chemical process of the Sol-gel process.

In Figure 4.2 above the basic chemical process for the formation of the Sol-gel is shown. A colourless liquid called Tetraethoxyorthosilane (TEOS) is mixed with water. When an acid - in this case HCl - is mixed with this solution Silicic acid and Ethanol are produced.

There are two basic reactions place and it is these reactions that are at the basis of the Sol-gel process.

$$M - X + H_2O \longrightarrow M - OH + HX \quad .....4.1$$

$$M - OH + X - M \longrightarrow M - O - M + HX \quad .....4.2$$

$$M - OH + OH - M \longrightarrow M - O - M + H_2O \quad .....4.3$$

where M = metal or Si ; X = reactive ligand like halogen, OR, NR_2 . These equations are left in general form.

Equation 4.1 represents the first reaction *hydrolysis* and equations 4.2 and 4.3 represent the *condensation polymerisation* reactions. By repetitive combinations of hydrolysis and condensation the gel structure is built up. The molecules start to form microscopic clusters which in turn coagulate to form larger entities finally building up into a coherent gel body. The fluorescent dye is added at the precursor stage ie. during the mixing of the initial solutions.

The overall pH of the solution and the ratio of water to TEOS are very important in controlling the rate at which hydrolysis and condensation polymerisation take place. The final stage is a heat treatment process to further densify the gel body so that it becomes a more permanent structure. In this work, this process lasted approximately 24 hours at a temperature of 73° C. More densified glasses are obtained by curing at higher temperatures (300-800 °C).

The treatment used in this work results in a material which has many advantages:

(a) it can be formed as easily as most glass-like transparent materials,

(b) it can be formed at low temperatures,

(c) one can incorporate foreign entities into the gel structure without changing the parameters of the Sol-gel process,

(d) one can deposit coatings on any surface at low temperatures,

(e) the material is homogeneous both at a macroscopic and at a microscopic level.

4.3 Coating of the Fibres

The etched fibres described in Chapter 3 were coated with Sol-gel at Trinity College Dublin by Mr.B.O'Kelly. His technique is shown in Figure 4.3 below.

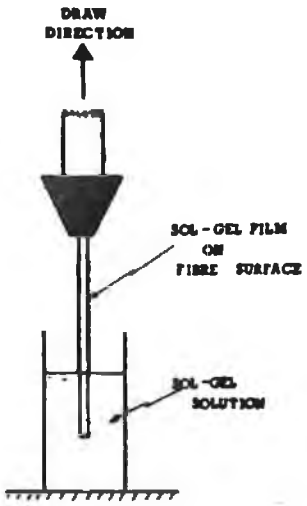

Figure 4.3 Diagram of fibre coating system.

The coating procedure involves three steps dipping,withdrawing and heating. The fibre is simply lowered into the Sol-gel solution and is then removed at a constant rate from the solution. The fibre is then left with a Sol-gel coating on its cylindrical surface and at the fibre tip. A typical film thickness was found to be in the order of 0.1 to 0.3 μm.Control of the film thickness is critical.If the Sol-gel film is too thick the coherent forces (forces which act within the film to minimize the film volume) cause shrinkage in a direction parallel to the circular plane of the fibre surface. If this coherent force is greater than the bonding of the film to the fibre surface then the film will completely or partially peel off. This peeling action is enhanced during the heating process and will eventually destroy the film. It is thought that for thin films the bonding force is so great that the films have less tendency to crack or peel off. For thin films such as the Sol-gel coatings used in this

project the film shrinks during the heat treatment perpendicularly to the fibre surface. The result is the formation of a film that bonds firmly to the fibre surface.

There are various factors affecting the thickness of the film:

(a) The *viscosity* of the coating:

The thickness of the film coating increases with the viscosity of the solution. The solution is rheopectic (the harder the liquid is stirred the more viscous it becomes) in nature. Therefore careful control of the mixing conditions of the solution is vital in producing a uniform coating. The thickness is proportional to the square root of the viscosity of the solution.

(b) The *rate of withdrawal*:

Because the solution has a rheopectic nature a faster withdrawal rate will result in a thicker film on the surface of the fibre. The thickness is proportional to the square root of the rate of withdrawal.

(c) The *oxide concentration* of the solution:

The dependance of thickness on the oxide concentration arises from the importance of the ratio of water to oxide concentration. For higher ratios of water to oxide concentration the greater the hydrolysis according to equation 4.1 .Brinker et al [35] explained that when this ratio is less than 4 the alcohol-producing condensation mechanism is favoured. When this ratio is greater than 4 the water producing mechanism is favoured. The growth of the Sol-gel is dictated by these two reactions namely equations 4.1,4.2 and 4.3. The thickness is found to be dependant on the square root of the oxide concentration [34].

(d)*Heating Temperature and time*:

During the heating process the Sol-gel undergoes shrinkage. The temperature and the amount of time heat is applied will determine the final thickness of the film.

To obtain thicker films one cannot dip the fibre into a Sol-gel solution several times- this would result in an unstable thicker coating. When these coatings undergo heat treatment the action of the coherent forces within the film cause cracking and eventual peeling. Therefore to achieve a thick coat one must dip the fibre once and then heat treat the fibre. Then re-dip the fibre with further heat treatment. In such a way a thick permanent layer is built up.

4.4 Ageing of Sol-gel Coatings

All of the Sol-gel coated fibres were checked for signs of ageing. A fibre which has been exposed to aqueous conditions greater than 50 times is shown in Figure 4.4. In Figure 4.5 a fibre which has been exposed to aqueous conditions less than 20 times is shown.

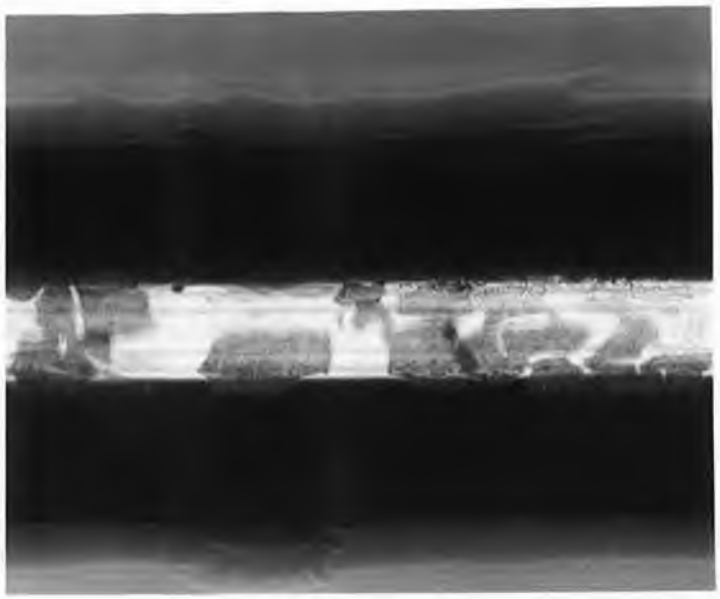

Figure 4.4 Picture of Sol-gel coated fibre- 5 months old.

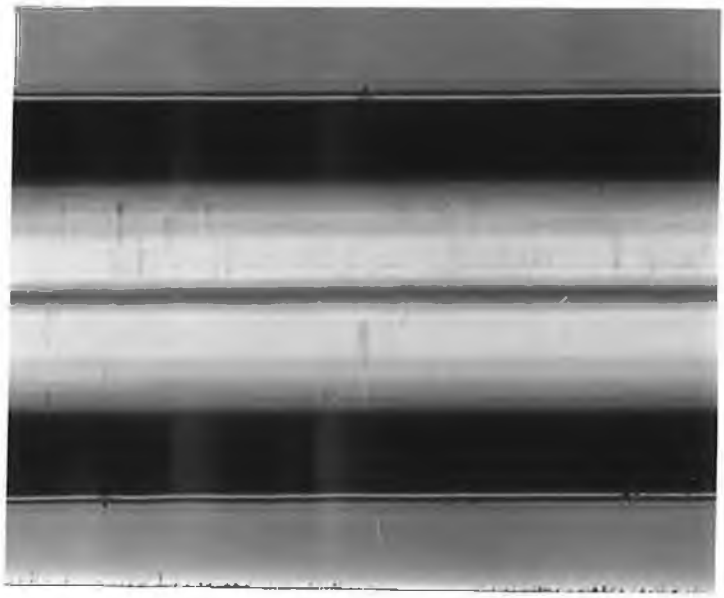

Figure 4.5 Picture of Sol-gel coated fibre- 1 week old.

Comparing these two examples one can observe that in the long term the Sol-gel coating tends to peel off but in the short term the film remains intact over many exposures to aqueous conditions. In Figure 4.4 one can observe that the Sol-gel coating is peeling off the surface of the fibre and when scraped with a knife the Sol-gel does offer some resistance to the scrapping action. This suggests that even after some months there is still a bonding force present in the Sol-gel coating.

A bulk sample of Sol-gel was made and was placed in water to investigate its stability. The sample was a disc of diameter 10 mm and 2 mm thick. The surface tension of the water caused the sample to shatter into very small fragments which in turn shattered again into thin flakes of gel; the smallest of which is less than 1 μm thick. Because the structural bonding forces are weaker for thicker Sol-gels the Sol-gel shattered and this was caused by the surface tension of the water. It is thought that when the Sol-gel pieces reached a size that was in equilibrium with the water in terms of forces the shattering stopped.The size of the remaining Sol-gel pieces were quite small - typically less than 1 μm - suggesting that the thinner the Sol-gel is the better its performance in aqueous conditions.

Other ageing processes that are present within the Sol-gel structure are polymerisation and shrinkage [33]. Polymerisation is the increase in the connectivity of the Sol-gel network produced by the condensation reactions outlined in equations 4.2 and 4.3. This results in less volume taken up by the gel matrix and a collapse of the Sol-gel network occurs.

Shrinkage is a phase transformation which results in the expulsion of liquid from the pores of the Sol-gel.This happens very slowly and becomes an obvious effect over a period of months. Both of these effects and long term exposure to aqueous conditions will reduce the surface area of the Sol-gel coating on the fibre until the bonding

force is broken and cracking results.

CHAPTER 5

EXPERIMENTAL RESULTS

5.1 Introduction

The experimental results of evanescently excited fluorescence in dye solutions in the environment of fibre probes is discussed. Three different solution geometries are described:

(a) the dye surrounding an unclad fibre probe,

(b) the dye chemically immobilised on the Silica core surface,

(c) the dye entrapped in a Sol-gel glass coated onto an unclad fibre.

5.2 Plain Evanescent wave probes in dye solutions

A 'plain probe' is simply a fibre whose primary coating and cladding layers are removed leaving the bare (plain) core.

The variation of evanescently excited fluorescence with:

(1) immersion depth (or interaction length)

(2) dye concentration

at different laser powers is discussed in this section. The experimental apparatus is shown in Figure 3.1 and the horizontal configuration of Figure 3.2(a) was used. Because standard fibre optic cleaving tools are not available for such large diameter fibres, a polishing technique was employed to achieve a good quality fibre end-face. A 4m long piece of Plastic Clad Silica (PCS) fibre of core diameter 600μm was polished at both ends using the polishing system described in Figure 3.7. One end of the fibre has its protective coating removed for approximately 25cms.

This exposed the cladding which was removed using the etchant described in Chapter 3. An opaque coating was made by mixing photocopier toner power in Araldite epoxy. The tip of the etched fibre was dipped into the solution and

left to harden. The probe is shown in Figure 5.1.
The probe was then mounted vertically on a vernier scale and the other end of the fibre was clamped to the micropositioner.

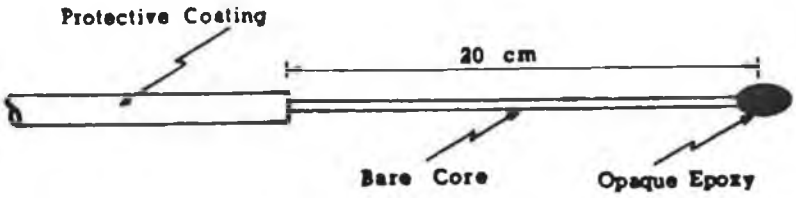

Figure 5.1 Diagram of an unclad fibre probe.

5.2.1 Immersion Depth Dependence

The purpose of this section was to verify the dependence of the intensity of the E.W. excited fluorescence on the immersion depth (the length L of the sensing volume $2\pi r d_p L$). The probe was placed vertically above a vessel of Rhodamine 6G diluted to a concentration of 10^{-3}M in ethanol. The probe head (see Figure 5.1) was lowered gradually into the dye-solution. A spectrum was recorded for each 5mm step for a total immersion depth of 65mm. This method was repeated for both immersion and extraction of the probe. A constant laser power of 13mW was used. A graph of the E.W. excited fluorescence against the depth of immersion and extraction was plotted and is shown in Figure 5.2.

From this Figure it is clear that the intensity of fluorescence increases linearly with immersion depth. This result is in agreement with the predictions of Equation 2.9 which predicts that $I_f \propto L$ where L is the immersion depth. The data is also in agreement with similar work of Newby [5]. The intensity of fluorescence for the extraction case decreases with decreasing L, but displays a non-linear behaviour. The difference in intensity, between the increasing immersion depth value and the corresponding extraction depth value is from photobleaching of the Rhodamine 6G dye.

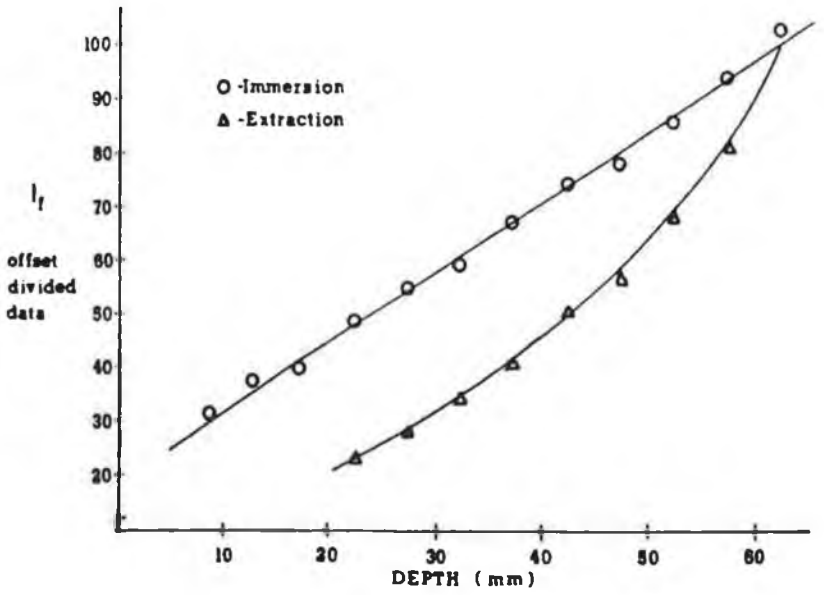

Figure 5.2 Graph of the intensity of fluorescence I_f against depth for immersion and extraction.

5.2.2. Concentration Dependence

The purpose of this work was to investigate the relationship between the intensity of fluorescence and the dye concentration for the case of E.W. excitation of fluorescence.

For this purpose a range of concentrations from 10^{-3}M to 10^{-5}M of Rhodamine 6G in Ethanol was made. The immersion depth was kept constant for this experiment. To keep the amount of photo-bleaching to a minimum a mechanically operated shutter was used to block the laser beam when not taking readings. The monochromator was set to a wavelength of 550 nm for all of the fluorescent intensity readings. The dye was exposed to laser light for 10s for each reading. Starting at the lowest concentration of 10^{-5}M the laser power was varied from 1 to 15 mW. This method was repeated for each concentration value. A graph of fluorescence intensity versus the concentration of Rhodamine 6G in ethanol for different laser powers is shown in Figure 5.3 .

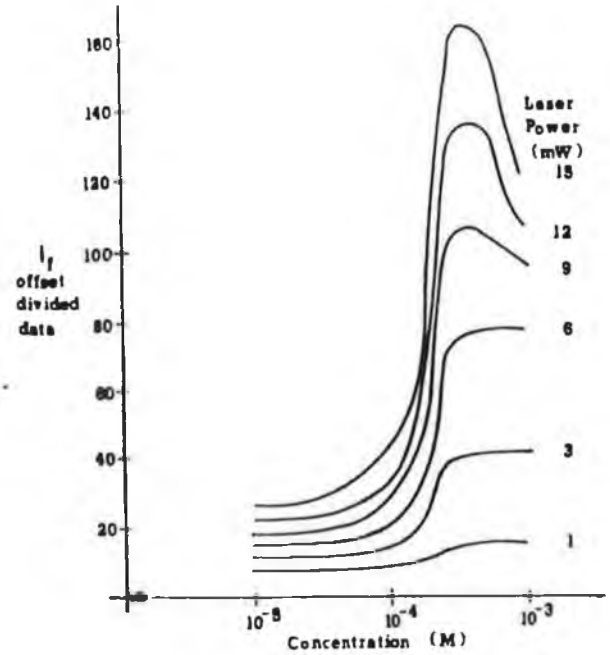

Figure 5.3 Graph of the intensity of fluorescence I_f against concentration for different laser powers.

For laser powers of less than 6mW, the intensity of fluorescence was found to saturate at a concentration of 10^{-3}M. For laser powers greater than 6mW , the intensity of fluorescence was found to exhibit a maximum at $5x10^{-4}$M which is independent of laser power. This indicates that the probe is most sensitive in the 10^{-4}M to 10^{-3}M region. In Figure 5.2, the fact that the curve exhibits a maximium indicates the presence of the inner filter effect. During the 10s exposure time, the intensity of fluorescence was observed to decay rapidly with time at higher laser powers indicating a high level of photobleaching.

5.3 Evanescent probes based on Chemically Immobilised Dyes

Many optical sensors are based on chemically sensitive fluorescent dyes or fluorescently labelled species. For this reason it was decided to examine means of immobilising these dyes onto a silica core surface.

Because the dyes cannot bind directly onto the core, surface modification or 'activation' of the core surface was required. The activation layer is normally achieved with reagents of the type $(RO)_3Si-R$, where R can be 3-aminopropyl, 3-chloropropyl, 3-glycidyloxy, vinyl or a long chain amine. The immobilisation of the dye then occurs by covalent binding between the functional group R and the dye.It was decided to work with short lengths of fibres (90mm) so that testing of each technique would be easier and conversion to a more practical disposable tip sensor could be achieved.

Various immobilisation techniques to attach the dyes

Fluorescein Isothyocyanate (FITC), and

Fluoresceinamine

to silica fibre cores were investigated by Dr.P.Greer and Mr. P.Eustace at Dundalk Regional Technical College. The immobilisation techniques are listed (by activation layer type) in Table 5.1. For each immobilisation technique 10 rods were prepared using the cladding removal method outlined in Chapter 3. This was performed by us at D.C.U. and these samples were then sent to Dundalk R.T.C. for immobilisation.

The apparatus used to investigate the probes is shown in Figure 3.1 and the horizontal configuration shown in Figure 3.2(a) was used together with a Knife-edge fibre support. For each fibre a spectrum was recorded from 505nm to 585nm. Each batch was then evaluated for fluorescence intensity, peak wavelength, optical emission spectrum and consistency between fibres produced in one batch. This involved the recording and analysis of over 100 spectra. Because this data contained great variability in terms of signal to noise ratio and batch consistency, the individual fibre data has not been included. However, a summary table of immobilisation methods together with their optical performances are listed in Table 5.1.
A typical FITC scan is shown in Figure 5.4 showing the optical parameters that were examined.

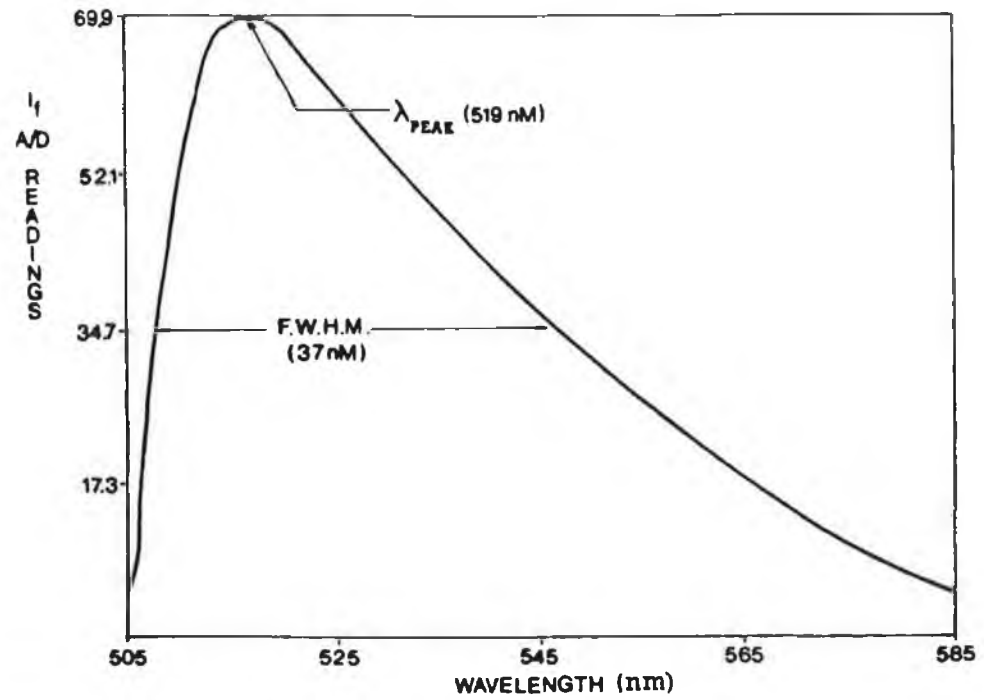

Figure 5.4 Typical FITC spectrum showing the required optical parameters.

Immobilisation Technique	Dye Type	Signal to Noise Ratio	λpeak Consistency	Spectral Shape
Amino Silane	A	V. low	Varied	Not Consistent
Glutaraldehyde	B	V. low	Varied	(as above)
Dihydrazide	A	High	Good 528nm	Consistent
Acyl Azide	B	Low	Varied	Not Consistent
Pararosaniline	A	Low	Varied	(as above)
Succinic Anhydride	B	Low	Varied	Consistent
Acyl Chloride	B	V. low	Varied	Not Consistent
Cyanuric Chloride	B	Medium	Good 515nm	Consistent
Rosolic Acid	B	Low	Varied	Not Consistent
HomoCysteine Thiolactone	A	High	Good 530nm	Consistent

Table 5.1 Evaluation results of the Immobilisation Techniques for FITC (A) and Fluoresceinamine (B) dyes.

The most successful immobilisation techniques that had a strong signal, consistent peak wavelength and spectral shape were found to be:

a)Dihydrazide with FITC

b)Cyanuric Chloride with Fluoresceinamine

c)HomoCysteine Thiolactone with FITC

Although three immobilisation techniques were found to have relatively high signals, each displayed a significant variance about their average detected signal level. The statistical variance values are 33.4%, 27.8% and 36.5% for techniques a), b) and c) respectively. In other batches various dye concentrations were investigated but the measured fluorescence exhibited no direct dependence on the concentration.
Consequently these techniques are limited in their potential for large scale production of fluorescence sensors, firstly because of their inconsistent batch signal levels and secondly, the inconsistency of the signal level with dye concentration suggests that an attempt at internal referencing would be difficult to achieve.

Because FITC and Fluoresceinamine are dyes whose fluorescence is known to be dependent on the pH of their local environment, it was decided to test some of the more successful chemically immobilised fibres for their pH sensitivity.A flow cell and fibre mount was designed to expose the fibre to a range of pH buffers (pH2 to pH7). The monochromator was set to the peak emission wavelength of each dye and each fibre was exposed in turn to the pH buffers.

A change in the intensity of fluorescence was not observed. It is not clear exactly why these methods were unsucessful but other workers in this field recommend using commercial 'ready to use' immobilised dye complexes rather than self-prepared immobilisation material. The former material is available in continuous quality whereas the material produced in the laboratory on a small

scale varies from preparation to preparation[43].

The inhibition of pH sensitivity together with the large batch variability motivated a search for other coating techniques, one of which is discussed in the next section

5.4 Dye Impregnated Sol-Gel coated probes

As described in Chapter 4, porous glass coatings formed by the Sol-gel technique are particularly attractive for optical fibre sensor applications because:

1) the compatibility with the SiO_2 surface, and
2) the high specific area providing many binding sites for the chemically sensitive dyes.

Various dyes were entrapped using the Sol-gel technique described earlier. Unclad fibres were prepared at DCU and were then sent to Trinity College Dublin (TCD) where the Sol-gel coatings were applied by Dr.J.McGilp and Mr.B.O'Kelly.

To achieve the most efficient coating technique, testing of the fibres, subject to a range of coating methods, was carried out here in this laboratory. These results were discussed in detail with the TCD group in the initial stages. The coating technique adopted for this work is described in Chapter 4. For all of the fibres the fluorescence intensity, peak wavelength, and spectral consistency were investigated. This involved the recording and analysis of over 150 spectra. E.W. excited fluorescence spectra for three dyes (FITC, fluorescein and rhodamine 6G) are shown in Figure 5.5.

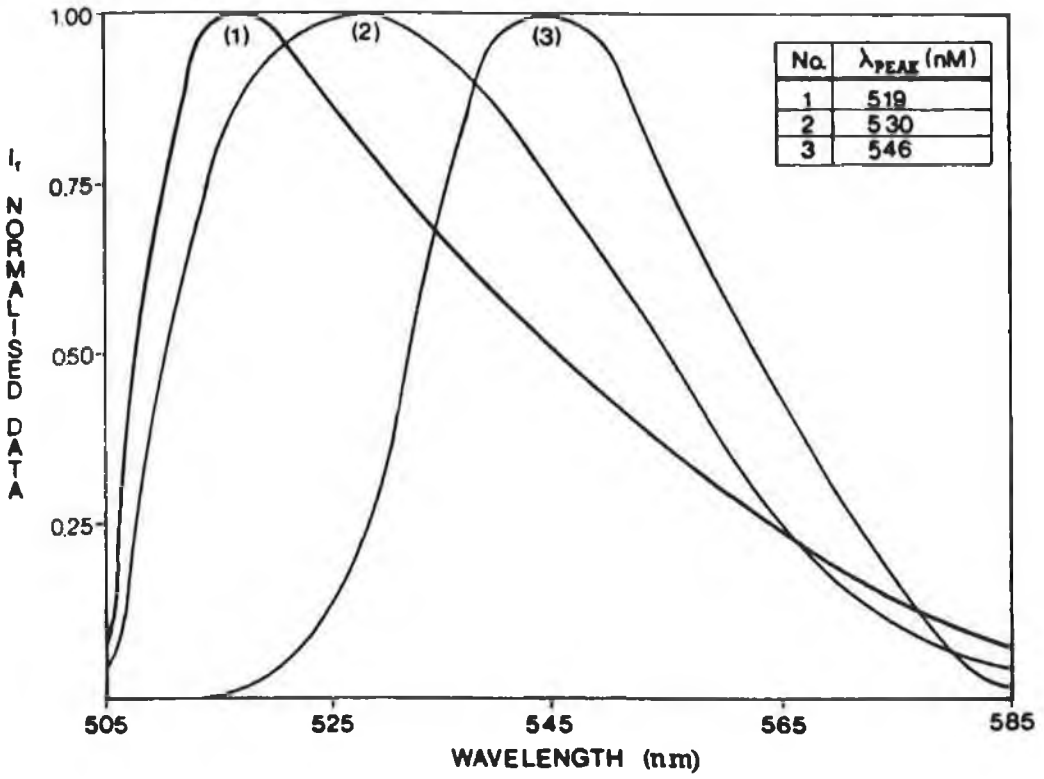

Figure 5.5 Diagram showing three dye spectra.
(1) FITC
(2) Fluorescein
(3) Rhodamine 6G

Fluorescein isothyocyanate (FITC) was found to have the lowest peak wavelength of 519nm and has a much sharper peak than Fluorescein or Rhodamine 6G. Fluorescein and Rhodamine 6G have very similar spectral shape but differ in terms of their peak wavelengths which were found to be 530nm and 546nm, respectively. These are roughly 20nm shifted towards the blue end of the spectrum in comparison with bulk fluorescence spectra and have a similar spectral shape in comparison to the bulk case.

5.4.1 Dye Concentration

An investigation of the relationship between the dye concentration and the E.W. excited intensity of fluorescence was carried out. A batch of rods with different dye concentrations in the Sol-gel coating was prepared. Each rod in turn was placed into the apparatus and scanned from 505nm to 585nm. The results are shown in Figure 5.6.

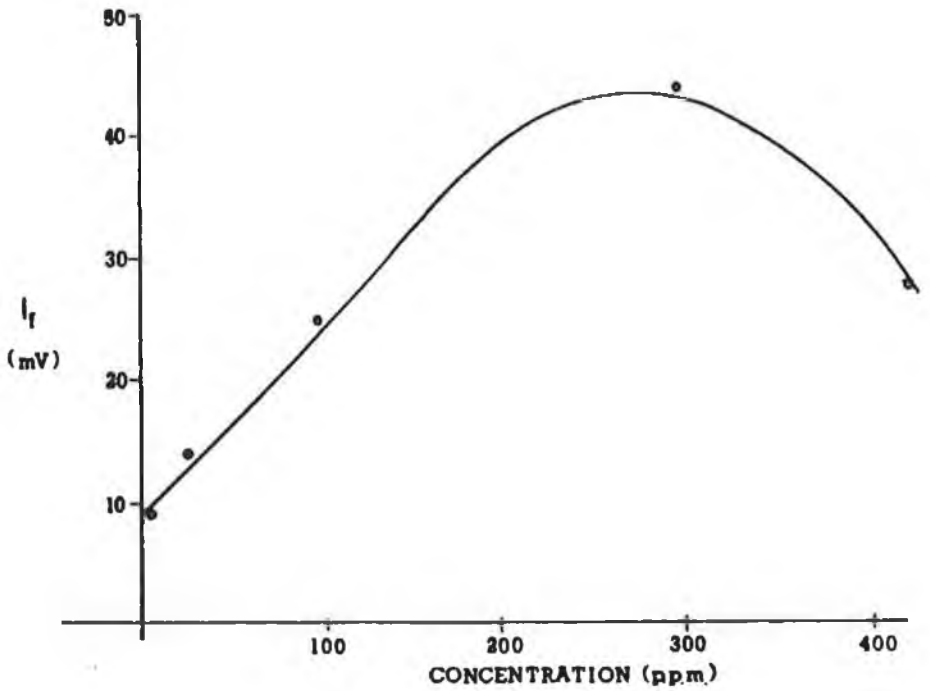

Figure 5.6 Graph of the intensity of fluorescence I_f against concentration for Sol-gel coated fibres.

These results show conclusively that there is an optimum value for the dye concentration at which the E.W. excited fluorescence intensity is a maximum. The decrease in intensity at higher concentrations is chiefly caused by the inner filter effect. This effect has been reported by Newby [5]. A similar relationship exists between the intensity of fluorescence and the dye concentration in the bulk case (see Figure 1.3).

A batch of fibres with the same dye concentration (100 ppm - the concentration values are given on a weight ratio of the amount dye to silica present in the precursor solution) within the Sol-gel was prepared to investigate the consistency of the technique. Qualities such as the intensity of fluorescence, peak wavelength, and spectral consistency were investigated. Results showed that there was a consistent spectral shape and peak wavelength.The variance in the detected fluorescence intensity was found to be less than 10% of the average fluorescence intensity which is a much better degree of consistency than that of the chemical immobilisation technique.

5.4.2 Photobleaching of the entrapped dye

The Photo-bleaching process is described in Chapter 1. The effect gives rise to a decreasing fluorescence signal over time. An experiment was carried out to find the relationship between the rate of decay of the fluorescence signal and the laser power.

A Sol-gel coated fibre was placed in the system described in hFigure 3.2(b). The monochromator was set to λ = 550nm (the wavelength maximum of the dichroic filter) and the laser power was reduced to 4 mW. The fibre was then exposed to a range of laser powers (4mW to 9mW). The exposure time was 2 minutes for each laser power.

The results are shown in Figure 5.7

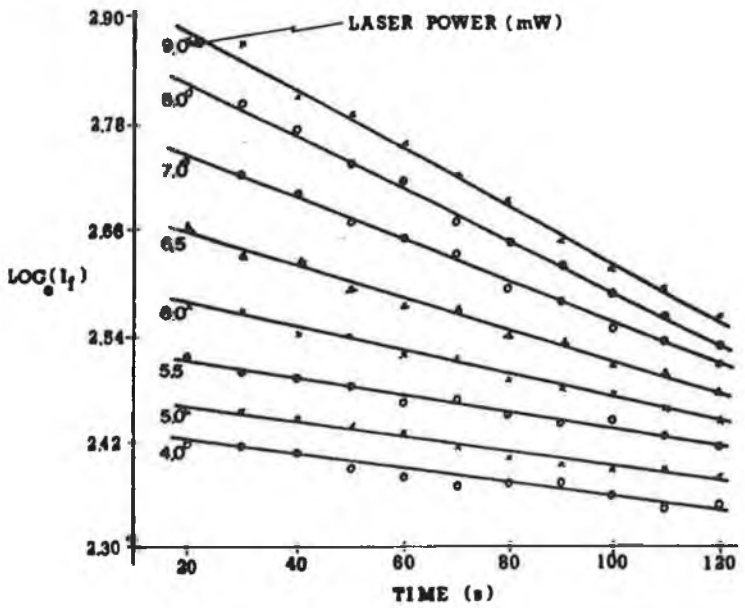

Figure 5.7 Graph of the intensity of fluorescence I_f with time for different laser powers.

This experiment was carried out for several different dyes entrapped in the Sol-gel. It is well known that the rate of decay is power dependent. Photobleaching, whose nature is not fully understood [45] is an unavoidable problem when dealing with fluorescent dyes. In the case of optical sensors based on such dyes the problem can be

minimised by using low excitation power and high signal amplification.

5.4.3. Investigation of Probe pH Sensitivity

Fluorescein and its derivatives are well known to have pH-dependent fluorescence. An E.W. sensor based on the pH sensitivity of fluorescein was investigated. Fluoresecein was entrapped in a Sol-gel which was coated onto the surface of an unclad fibre. A number of such fibres was then investigated for their response to changes in the local pH environment. The apparatus used to examine the fibres for pH sensitivity was based on the system shown in Figure 3.2(b). The Sol-gel coating was confined to the lower 3 cm of the unclad fibre probe to ensure that the sensing region (defined by the Sol-gel coating) was totally immersed in the fluid. Previous experiments had shown that fluctuations in the fluid level along the sensing region had caused intensity changes. The probe was mounted in the system and the sensor was exposed in turn to a range of pH buffers from pH2 to pH6.5 . The pH buffer was stirred throughout the duration of the experiment. The monochromator was set to 530nm, the peak emission wavelength for fluorescein. Starting from pH2, the pH was increased in steps of 0.5 pH units until pH6.5 was reached. Then the pH was decreased by the same step size down to pH2. The above was repeated several times for a range of laser powers.

In Figure 5.8 the step changes in the intensity of fluorescence signal over a pH range from 3.5 to 6.5 is illustrated for laser powers of 6mW and3mW respectively. There is significant photo-bleaching occurring at a laser power of 6mW but at a laser power of 3 mW the amount of photo-bleaching is reduced. A full description of the performance of the pH probe is given in the next section.

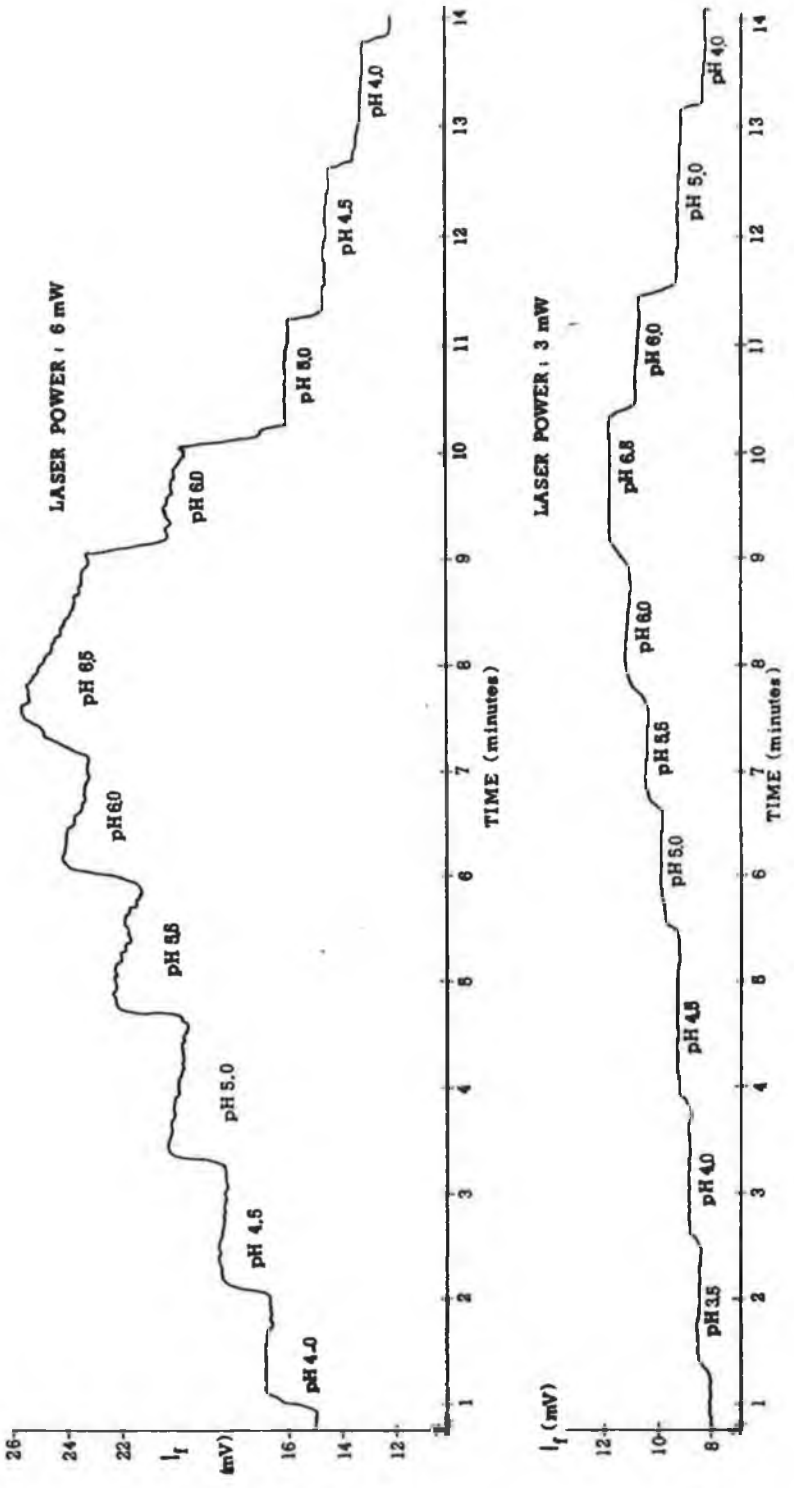

Figure 5.8 Graph of the intensity of fluorescence I_f against the pH of the local probe environment.

(Time is shown to indicate the duration of the pH test.)

5.4.4 Characterisation of the pH Probe

The motivation for using fluorescein in the porous Sol-gel coating was to evaluate the general potential of this probe configuration as a sensor. Because of the inherent porosity of the Sol-gel its main application will be in gas sensing- future developments are discussed in Chapter 6.

The probe developed in this work , using fluorescein as a pH indicator, can be described by the following characteristics:

(a) Reversibility
(b) Response Time
(c) Sensitivity
(d) Stability

(a) Reversibility.

Due to photon-bleaching of the fluorescent dye the probe suffers from a lack of reversibility as shown in Figure 5.8. There are two possible solutions to the problem:

1.Lower excitation powers can be used with a more sensitive detection system such as offered by photo-counting.

2.A second dye mixed with fluorescein can be used as an internal reference. This dye will bleach at the same rate as the sensing dye but will not respond to its local environment. In this way the ratio of the fluorescence signal from the sensor dye to that from the reference dye will yield a number which is a direct measure of pH but independent of photobleaching. This approach will be pursued in further work.

(b) Response Time.

The response time (defined as that time for the sensor to react to a change in its environment and reach a

constant intensity of fluorescence) is limited by the mass transfer of hydrogen through the Sol-gel matrix to react with the fluorophore. The response time was found to be approximately 5s. This is lower than that of Fuh et al (20s - 35s)[12] and is greater than that of Kawabata et al (1s) [18].

(c) Sensitivity.

In Figure 5.9 a graph of the evanescently excited fluorescence against pH is plotted.

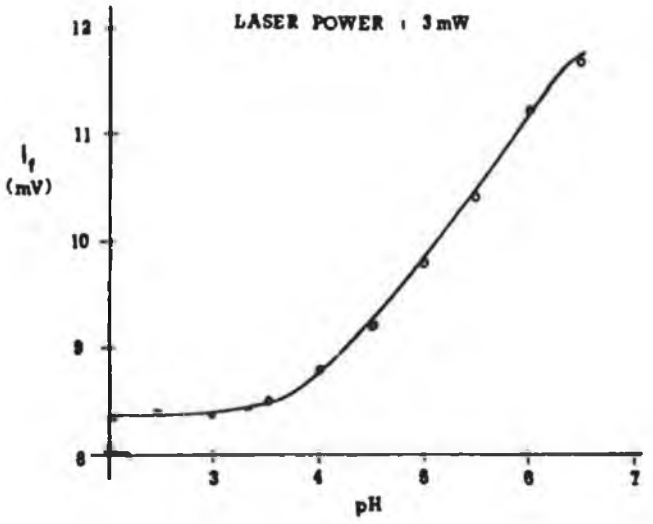

Figure 5.9 Graph of the intensity of fluoresence I_f against pH.

The pH range of the fluorescent dye was investigated in the range from pH2 to pH6.5 and was found to be most sensitive in the range of pH3.0 to pH6.5.

In addition a batch of fibres with various fluorescein concentrations within the Sol-gel was tested for pH response. The sensitivity of these fibres was expressed in terms of the percentage change in the fluorescent signal between pH2 and pH6. The results are shown in table 5.2.

Dye Concentration (p.p.m.)	% difference in fluorescence (pH2 to pH6)
>300	14
300	54
100	43
30	20
10	16

Table 5.2 Showing the relationship between Dye Concentration the % difference in fluorescence .

The dye concentration is given on a weight ratio of the amount dye to silica present in the precursor solution. The maximium value of the dye concentration was greater than 300 ppm. The actual value can not be specified because at concentration values of 400ppm or greater the dye did not disolve readily to yield a clear solution. These results suggest an optimium dye concentration for maximum pH sensitivity. The optimium value for the dye concentration occurs in the region 100ppm to 300ppm. Future experiments will investigate this dependence more rigorously.

(d) Stability.

Badini et al [19] reported the existence of a *washout* effect in a similar pH sensor. Their sensor configuration was a tip-coated fibre in which a pH sensitive dye (FITC) was incorporated into a polyemetric matrix on the end-face of an optical fibre. The sensor suffered from the dye being washed out of the matrix each time it was in contact with aqueous conditions.

Three of the sol-gel coated fibres used in this work were washed for the period of a week. During this period the water used to wash the fibres was analysed using a fluorimeter. There was no dye detected in the water showing that there was no significant washout effect with the Sol-gel technique.

5.4.5 The Dependence of Fluorescent Intensity on V-number

During the course of experimentation it was observed that the intensity of fluorescence changed when the probes environment was changed from air to water. Experimental data was taken for these two situations and is shown in Figure 5.10. The decay seen here is due to dye photo-bleaching. The region of interest is at the air/water transition where there is a sharp decrease in Fluorescence.

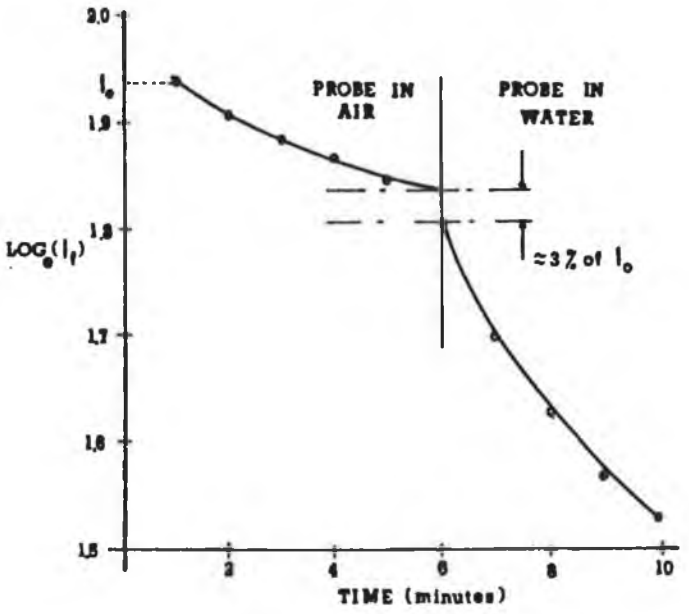

Figure 5.10 Graph of $Log_e I_f$ against time in an air and water environment.

As explained in equation 1.2 the V-number of a fibre is directly proportional to $\sqrt{n_1^2 - n_2^2}$ (n_1 and n_2 being the core and cladding indices, respectively). For a weakly guiding fibre ($n_1 \approx n_2$) the V-number is small and the fractional optical power in the cladding (shown by Gloge to be $4\sqrt{2}$ / 3V [39]) is large. As shown in equation 1.4 earlier the fluorescent intensity

I_f is directly proportional to the excitation power which implies that the observed fluorescent power in a fibre due to E.W. excited fluorescence in the cladding should *increase* with decreasing V-number. Thus for example an unclad silica fibre with a dye immobilised on its surface should exhibit weaker fluorescence when located in air with $V_1 \propto \sqrt{n_1^2 - 1}$ than when surrounded by water with $V_2 \propto \sqrt{n_1^2 - (1.33)^2}$, since $V_1 > V_2$. The behaviour in the air/water transition region illustrated in Figure 5.10 is in direct conflict with this theory. Thompson and Kondracki [38] have observed recently that the fluorescence collection efficiency for E.W. excited fluorescence increases with increasing V-number as shown in Figure 5.11 .

There are, therefore, two competing effects coming into play in the overall collection efficiency of E.W. excited fluorescence:

(1) excitation efficiency which is inversely proportional to V.

and (2) collection efficiency which increases with V.

Thompson and Kondracki [38] speculated that these conflicting dependences on the V-number should lead to an optimum V-number. This was in fact observed by them and is illustrated in Figure 5.12.

Marcuse [15] states that the coupling efficiency climbs as V^n where n >1. An analysis of his graph (Figure 5.11) yields a value of slightly less than 2 for n. As the excitation efficiency varies as V^{-1} the combined effect on the fluorescent intensity coupled back into the fibre scales as V^{n-1} i.e. increases with increasing V-number. This is consistent with our observation of a decrease in the detected fluorescence when the sensor is placed in water as illustrated in Figure 5.10.

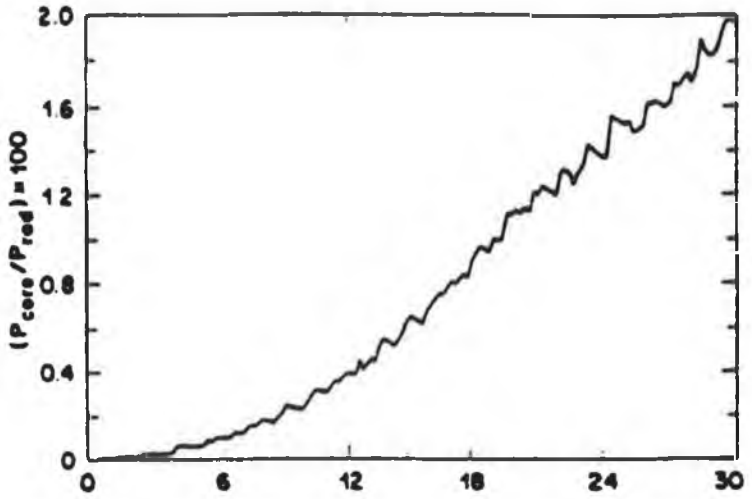

Figure 5.11 Graph of launch efficiency against the V-number - from Marcuse [15].

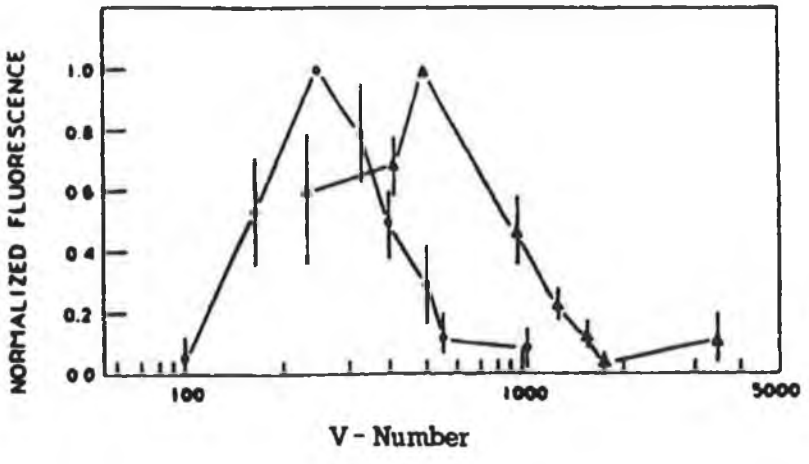

Figure 5.12 Dependance of fluorescence on V-number taken from Thompson and Kondracki [38].

5.5 Conclusion

Evanescent wave excitation of fluorescence was used in a number of configurations:

(1) at the distal end of an optical fibre,

(2) on a short length of unclad optical fibre with dye chemically immobilised on its surface,

(3) on a short length of unclad optical fibre with a Sol-gel entrapped dye coated onto the surface.

In the first configuration the variation of the intensity of fluorescence with interaction length and dye concentration was investigated. The results agree with the theory predicted in Chapters 1 and 2. Although this type of sensor is a good configuration for the analysis of evanescent wave effects it suffers from modal instability along the length of the fibre caused by such effects as microbending or a gradual loss of the critical angle condition in the sensing region when guided by a fully clad fibre.

In the second configuration, where chemically immobilised dyes on optical fibres were investigated, the results were poor in terms of the reproducibility of the coatings. Most of the techniques yielded low signal levels and the peak emission wavelength varied.

Finally, fluorescent dye located in the pores of a Sol-gel proved to be a successful method of achieving a good quality coating using the technique described in Chapter 4. The detected E.W. excited fluorescence on dye concentration was found to be very similar to that of bulk. The coatings were reproducible in terms of their optical parameters such as spectral shape, peak wavelength and fluorescence intensity.

A pH sensor was developed using this method with a pH sensitive dye entrapped by the Sol-gel technique. The sensitivity of the probe was found to be in the range of pH3.0 to pH6.5. The sensor has a relatively fast response time $\simeq$ 5s.

The disadvantage of both Chemical immobilisation and the Sol-gel method of attaching dyes is that both methods suffer from photo-bleaching which can be minimised using low incident laser power.

CHAPTER 6

CONCLUSION

An optical system was built to detect evanescent wave (E.W.) excited fluorescence from fluorescent dye molecules located near the core surface of an optical fibre. The design was based on the theoretical parameters outlined in the theory of E.W. excited fluorescence (Chapter 2).

The evanescent wave excitation of fluorescence in dyes located close to the surface of an unclad multimode step index fibre was examined in terms of the following variables:

Excitation power
Fibre interaction length
Fibre V-number
Dye concentration

The results of this work agree broadly with the theory outlined in Chapter 2. A number of chemical methods of immobilising fluorescent dyes directly onto the fibre core surface were investigated and none of these were found to be satisfactory. Problems associated with these methods included inconsistent emission spectra, peak wavelength variation, optical instability in terms of photo-bleaching, large batch variations and generally a low signal to noise ratio under E.W. excitation.

The coating of an optical fibre core surface with a porous glass doped with fluorescent dye molecules was found to have potential in fibre optic fluorescence sensors. This process involved coating the fibre with a thin glassy layer formed by the sol-gel process. Preliminary results showed that such coatings are easily reproducible. Within a batch of fibres the same peak wavelength, spectral shape and intensity of fluorescence was achieved. There was a small variation in the intensity of fluorescence but this variation is much lower than for the immobilisation technique. Fluorescein is a well known pH indicator and was used as the dopant in the Sol-gel process to evaluate

the technique for its potential as a pH sensor. The probe was found to be most sensitive in the range pH3.0 to pH6.5.

This probe has applications in the medical field where, for example, the probe could be used to measure gastric fluid in young children (a pH range of 0 to 7). The probes size means that a design similar to the endoscope already used in this field could be used or the probe could be inserted through existing guiding tubes within the endoscope. Another application, in the future, using a low excitation power and single shot measurement is in the environmental area where acid rain could be measured.

Particular emphasis on a tip coating technique using the Sol-gel method where the Sol-gel is coated onto the distal end of an optical fibre is an important application and futher work is required to investigate this. In addition, the Sol-gel technique has particular potential for gas sensing, making use of its porosity and high specific area. This technique has also an application in continuous distributive sensing where, for example, prolonged measurement of oxygen can be achieved using a Ruthenium complex as a dopant.

REFERENCES

[1] T.G. Giallorenzi, J.A. Bucaro, A. Dandridge and J.H.Cole, I.E.E.E. Spectrum, Sept. (1986) p45

[2] S.M. Angel
Spectroscopy, **2** (4) (1987) p38

[3] J.F. Place, R.M. Sutherland and C. Dähne,
Biosensors, **1**, (1985), p321

[4] W.M. Reichert, P.A. Suci, J.T. Ives and J.D.Andrade
Appl. Spec. **41**(3), (1987), p503

[5] K.E. Newby
Thesis submitted to the Univ. of Utah for the degree of M.Sc.. Dec 1984

[6] O.S. Wolfbeis
Trends in Anal. Chem., **2**(8), (1983), p176

[7] R.A.Badley, R.A.Drake, I.A.Shanks, A.M.Smith, and P.R.Stephenson, Phil. Trans. R.Soc. Lond., **B316**, (1987)

[8] R. Kooyman, H. de Bruijn, and J. Greve
Proc. SPIE **789** (1987) The Hague.

[9] R. Lieberman, L. Blyler and L. Cohen
Opt. Soc. of Am., Tech. Dig., **2**, (1988), p346

[10] O.S. Wolfbeis, L.J. Weis, M.J.P. Leiner and W.E. Ziegler, Anal. Chem. **60**, (1988), p2028

[11] C.K. Carniglia, L. Mandel and K.H. Drexhage,
J.Opt.Soc.Am., **62**(4), (1972), p479

[12] M.R. Fuh, L.W. Burgess and G.D. Christian
Anal. Chem., **112**, (1987), p1159

[13] R.M. Sutherland, C. Dähne and J.F. Place
Clin. Chem., **30**(9), (1984), p1533

[14] R.A. Lieberman, L. Blyler and L.G. Cohen
J. Lightwave Tech., **8**(3), (1990), p212

[15] D. Marcuse
J. Lightwave Tech., **6**(8), (1988), p1273

[16] W.F. Love and L.J. Button
Proc. SPIE **990**, Boston (1988).

[17] N.J. Harrick "Internal Reflection Spectroscopy"
John Wiley and Sons N.Y. (1967)

[18] Y. Kawabata, T. Imaska and N. Ishibashi
Proc. 4th Int. Conf. Optical Fibre Sensors OFS'86
Tokyo (1986)

[19] G.E. Badini, K.T.V. Grattan, A.W. Palmer
and A.C. Tseung, Proc. 6th Int. Conf. Optical Fibre
Sensors OFS'89 Paris (1989)

[20] A.Arie. R.Karoubi, Y.S.Gur and M.Tur
Appl. Opt., **25**(11), (1986) p1754

[21] D.R. Walt, C. Munkholm, D. Jordan, F.P. Milanovich
and F. Daley
Proc. SPIE **713**, Optical Fibres in Medicine **2**, (1986)

[22] J.I.Peterson, S.R. Goldstein and R.V.Fitzgerald
Anal. Chem., **52**(6), (1980) p864

[23] C. Munkholm, D.R. Walt, F.P. Milanovich
and S. Klainer, Anal. Chem., **58** (1986) p1427

[24] M.E. Cox and B. Dunn
Appl. Opt., **24**(14), (1985), p2114

[25] G.G.Guilbault
"Practical Fluorescence Theory, Methods
and Techniques" Marcel Dekker, N.Y. (1971)

[26] V.R. Kaufman and D. Levy.
J. Non-Cryst. Solids., **82**, (1986) p103

[27] F. Orgaz and H. Rawson
J. Non-Cryst. Solids., **82**, (1986) p57

[28] H. de Lambilly and L.C. Klein
SPIE **683** Infrared & Optical Transmitting Materials
(1986), p98

[29] T. Tanaka
Sci.Amer., **258**, May (1988)

[30] S.P. Mukherjee
J. Non-Cryst. Solids, **42**, (1980), p477

[31] J. Fricke
Sci. Amer., **258**, May (1988)

[32] R.C. Mehrotra,
Conference Proceedings from "Sol-gel Science and Technolo
Sao Carlos (SP) Brazil. August 1989.

[33] G.W. Scherer,
(Same as [32])

[34] S. Sakka,
(Same as [32])

[35] C.J. Brinker,
(Same as [32])
[36] A.W. Snyder and J.D. Love,
"Optical Waveguide Theory"
Chapman and Hall, N.Y. (1983) Eqn. 7-3
[37] R.B. Thompson and F.S. Ligler,
Fibre Optic Biosensor Technology
NRL Memorandum Report No. 6182 (1988)
[38] R.B. Thompson and L. Konchacki,
IEEE Eng. in Medicine.Biology Society 11th Annual
International Conference (1989) p1102
[39] D. Gloge,
Appl. Opt., 11(10), (1971) p2252
[40] J. Hecht,
"Understanding Fibre Optics."
H.W. Sans & Co. (1987)
[41] O.S. Wolfbeis, L.J. Weis, M.J.P.. Leiner
and W.E. Zeigler, Anal. Chem., 60, (1988) p2080
[42] J.D. Andrade, R.A. Van Wegener, D.E. Grepamis,
K. Newby and J.N. Lin,
IEEE Trans. Elect. Dev., 32(7), (1985) p1175
[43] O.S. Wolfbeis,
"Molecular Luminescence Spectroscopy: Methods and
Applications -Part II"
John Wiley and Sons (1988) pp 189
[44] V.Ruddy, B.MacCraith and J.Murphy,
J.Appl. Phys, 67(10), (1990), p6070
[45] T.W.Hänch, "Applications of dye lasers"
From "Dye lasers" Springer and Verlag, Berlin (1977)

ACKNOWLEDGEMENTS

The author wishes to thank Dr. Brian MacCraith and Dr. Vince Ruddy for their unlimited attention throughout the duration of this project.
Thanks go to Dr.Paddy Greer, Mr.Paul Eustace, Dr. John McGilp for the cooperation in the initial development of the work completed in this thesis. Very special thanks to Brendan O'Kelly for his work in making the Sol-gels.
Special thanks go to Simon and Adrian for their support while I was working beside them. Many thanks go to fellow postgrads who kept my mind off my work while I was working.

APPENDICES

Appendix A1

A brief description of the origin of the *EVANESCENT WAVE.*

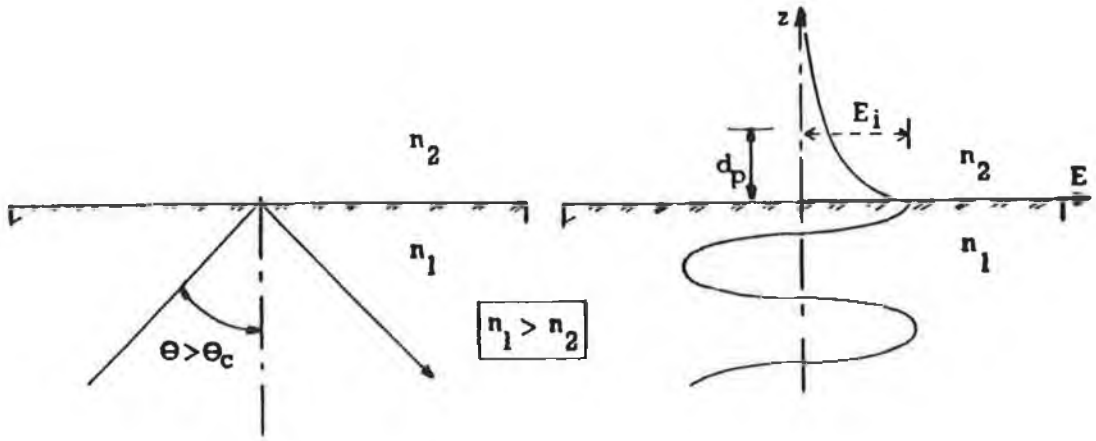

Figure A1 A diagram showing the generation of the evanescent wave at an interface between two media ($n_1 > n_2$)

In Figure A1, one can observe for an incoming ray incident at an interface between two media of refractive indices n_1 and n_2 that according to Snell's Law Total Internal Reflection (TIR) will occur.

When Maxwell's equations are applied to light waves approaching such an interface (for example, the core/cladding interface of an optical fibre) it can be shown that standing waves are established normal to the interface because of the superposition of the incoming and reflected waves and a non-propagating evanescent field is established in the rare medium.

To explain more clearly how this evanescent wave is formed consider the following:

If n_1 and n_2 are the refractive indices of the dense and rare medium respectively,

$$\Rightarrow \theta_c = \mathrm{Sin}^{-1}(n_2 / n_1) = \mathrm{Sin}^{-1}(n_{21}) \qquad \text{A1.1}$$

Adopting the exponential representation of a travelling wave ,

$$\vec{E} = \vec{E}_{int} \exp i\,(\vec{k}_t.\vec{r} - \omega t) \ldots\ldots\ldots\ldots A1.2$$

where $|\vec{E}_{int}|$ is the electric field amplitude at the interface.

If z is the direction into the rare medium perpendicular to the interface and y is the direction parallel to the interface then:

$$\vec{k}_t.\vec{r} = k_{ty}y + k_{tz}z$$

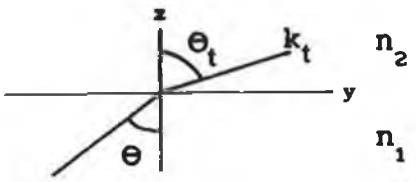

Therefore k_t represents the propagation vector within the rare medium at an angle of θ_t to the normal to the interface.

$$\Rightarrow k_{ty} = k_t \text{ Sin } \theta_t \qquad \& \qquad k_{tz} = k_t \text{ Cos } \theta_t$$

Concentrating on the wave disturbance perpendicular to the interface ie k_{tz},

$$k_{tz} = k_t \text{ Cos } \theta_t = \mp k_t (1 - \text{Sin}^2\theta_t)^{1/2} \ldots\ldots A1.3$$

Using Snell's Law, ie $n_1 \text{Sin } \theta = n_2 \text{Sin } \theta_t$ equation A1.3 now reads as follows:

$$k_{tz} = \mp k_t \left(1 - \frac{\text{Sin}^2\theta}{n_{21}^2}\right)^{1/2}$$

Remember that for TIR, Sin θ > n_{21} therefore k_{tz} must be imaginary.

$$\Rightarrow k_{tz} = \mp i\, k_t \left(\frac{\text{Sin}^2\theta}{n_{21}^2} - 1\right)^{1/2} = \mp i\,\delta \ldots\ldots A1.4$$

Using Snell's Law, $k_{ty} = k_t \text{Sin } \theta_t$

$$= k_t \frac{\text{Sin } \theta}{n_{21}} \quad \ldots\ldots\ldots\ldots\ldots \text{A1.5}$$

Equation A1.2 can be written in the following form:

$$E = E_{int} \exp i(k_{ty} + k_{tz} - \omega t)$$

Hence, combining equations A1.4 and A1.5 with the above equation, the equation now becomes:-

$$E = E_{int} \exp(-\delta z) \cdot \exp i(k_t y \frac{\text{Sin } \theta}{n_{21}} - \omega t)$$

The above equation describes a wave travelling parallel to the interface in the y direction and having a component in the rare medium decreasing exponentially with distance into the medium.

δ is given by:

$$\delta = k_t \left(\frac{\text{Sin}^2\theta}{n_{21}^2} - 1\right)^{1/2}$$

k_t is the wave number or scalar representation of the propagation vector in the rare medium and is given by,

$$k_t = \frac{2\pi n_2}{\lambda}$$

where λ is the free space wavelength.

Hence δ becomes $$\delta = \frac{2\pi n_2}{\lambda}\left[n_1^2 \frac{\mathrm{Sin}^2\theta}{n_2^2} - 1 \right]^{1/2}$$

$$= \frac{2\pi n_1}{\lambda}\left[\mathrm{Sin}^2\theta - n_{21}^2 \right]^{1/2}$$

We can now define the penetration depth as the distance required for the electric field amplitude to fall to 1/e of its value at the interface,

$$\text{i.e.,} \qquad e^{-\delta y} = e^{-1}$$

Hence, the penetration depth can be written as,

$$d_p = \frac{1}{\delta} = \frac{\lambda}{2\pi n_1\left(\mathrm{Sin}^2\theta - (n_2/n_1)^2 \right)^{1/2}}$$

where λ is the free space wavelength,

n_1 is the refractive index of the dense medium,

n_2 is the refractive index of the rare medium,

θ is the angle of incidence with respect to the normal to the interface.

From this expression, it can be seen that d_p gets large as θ approaches the critical angle θ_c and becomes infinite when $\theta = \theta_c$ meaning the light is no longer totally reflected and propagates across the interface.

Appendix A2 TRANSMISSION RESPONSE
FOR
THE DICHROIC FILTER

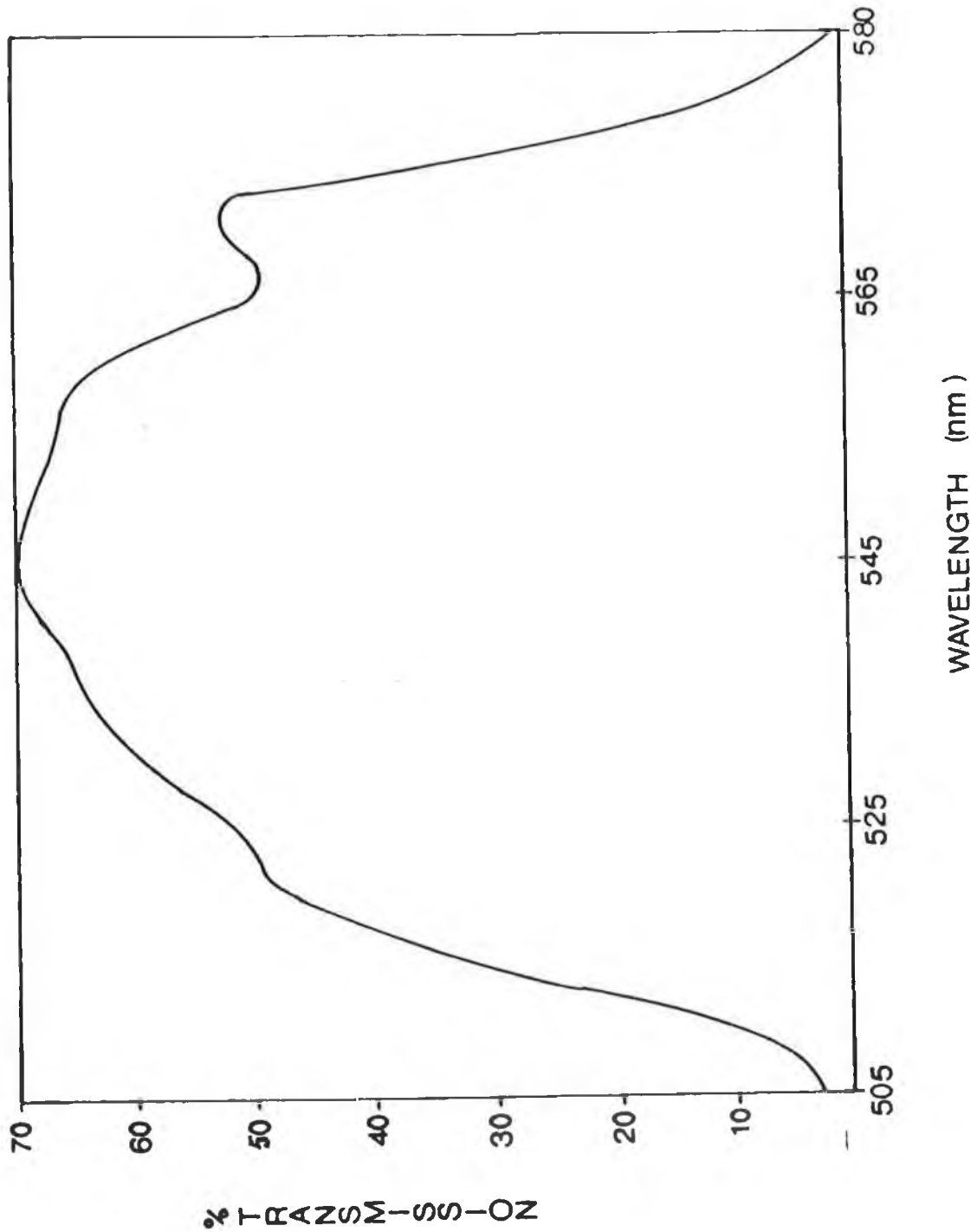

Appendix A3

Software.....Program 1 (System program)
Program 2 (System response generation)

Program 1

```
 10 REM    SLOWLINK PROGRAM
 20
 30 REM    MINICHROM MODEL 02
 40
 50 REM    WRITTEN BY K.DEVLIN
 60REM
 65 REM    ADAPTED BY C.POTTER
 70 CLS
 80 REM ********************************
 90 REM **                              **
100 REM ** PROGRAM TO CONTROL THE       **
110 REM **        MINICHROM             **
120 REM **        MODEL 02              **
130 REM **                              **
140 REM ********************************
150 MODE4
160 DIM Y(1000)
170 VDU15
180 YMAX=0:F=0
190 PRINT:PRINT
200 PROCMENU
210 DEF PROCMENU
220 PRINT TAB(12) "SOFTWARE OPTIONS"
230 PRINT TAB(12) "-------- -------"
235 PRINT:PRINT
240 PRINT TAB(8);"A"TAB(15);"DATA ACQUISITION":PRINT
250 PRINT TAB(8);"B"TAB(15);"DIVIDE BY REFERENCE":PRINT
260 PRINT TAB(8);"C"TAB(15);"PLOT GRAPH RIKADENKI":PRINT
270 PRINT TAB(8);"D"TAB(15);"SMOOTH DATA":PRINT
280 PRINT TAB(8);"E"TAB(15);"DISPLAY DATA FILES":PRINT
290 PRINT "INPUT OPTION LETTER ":N$=GET$
300 IF N$="A" THEN 345
310 IF N$="B" THEN CHAIN "DIVIDE"
320 IF N$="C" THEN CHAIN "RIKI"
330 IF N$="D" THEN CHAIN "SMOOTH"
340 IF N$="E" THEN *.
345 CLS
360 PRINT"SELECT FUNCTION:-"
370 PRINT:PRINT
380 PRINT TAB(12) "SET PARAMETERS    1"
390 PRINT TAB(12) "SET WAVELENGTH    2"
400 PRINT TAB(12) "SINGLE SCAN       3"
```

```
  410 PRINT TAB(12) "MANUAL SCAN        4"
  420 PRINT TAB(12) "SAVE DATA ON FILE 5"
  430 INPUT "SELECT OPTION";d
  440 IF d=1 GOTO 600
  450 IF d=2 GOTO 960
  460 IF d=3 GOTO 1330
  470 IF d=4 GOTO 1560
  480 IF d=5 GOTO 2140
  490 IF d<>1 GOTO 345
  500 REM ******************************
  510 REM *                            *
  520 REM * THE FOLLOWING PROGRAM      *
  530 REM * INTERFACES WITH THE CB1    *
  540 REM * CONTROLLER AND CHANGES ANY*
  550 REM * OF THE PARAMETERS          *
  560 REM*                            *
  570 REM ******************************
  580 VDU3
  590  MODE3
  600 PRINT:PRINT
  610PRINT "GO TO ZERO ORDER:TYPE G1"
  620 PRINT:PRINT
  630 PRINT "DO YOU WANT TO CHANGE:"
  640 PRINT:PRINT
  650 PRINT TAB(22) "DIVIDING FACTOR D"
  660 PRINT:PRINT
  670 PRINT TAB(22) "INITIAL VELOCITY I"
  680 *FX7,7
  690 REM RECEIVE BAUD RATE
  700 *FX8,7
  710 REM TRANSMIT BAUD RATE
  720 *FX229,1
  730 OSBYTE=&FFF4
  740 REM OSBYTE CALL
  750:
  760 L%=0
  770 FOR I1=1 TO 1000
  780 A%=138:X%=2:REM IE OSBYTE 138       135 REM RS423 O/P
BUFFER
  790 REM RS423 O/P BUFFER, INSERT INTO BUFFER
  800 *FX2,2
  810 IF ADVAL(-1)>0 AND ADVAL(-3)>0 Y%=GET:CALL OSBYTE
  820 *FX2,1
  830 REM GET CHAR FROM KBRD,ENABLE RX
  840 IF ADVAL(-2)>0 CHAR%=GET:VDU CHAR%:L%=L%+1
  850 REM CHECKS NO. OF CHARS IN KBRD BUFFER AND IN RS423
  860 IF L%=60 VDU10:VDU13:L%=0
  870 REM MOVE CURSOR TO NEW LINE
  880 NEXT
  890 :
  900 *FX2,2
  910 *FX229,0
  920 REM ESCAPE ENABLE
  930 *FX3,4
  940 Z=0
  950 GOTO 345
  960 CLS
```

```
 970 REM**************************
 980 REM*                        *
 990 REM* THE FOLLOWING SETS THE *
1000 REM* MONOCHROMATOR TO A     *
1010 REM* SPECIFIED WAVELENGTH   *
1020 REM*                        *
1030 REM**************************
1040 PRINT:PRINT
1050 INPUT "Wavelength position (nm)",W
1060 REM W<=6400 SETS THE MAXIMUM SCAN   TO 800nm
1070 W=W*8:IF W>=6400 THEN 1050
1080 IF W < F THEN 1160
1090 A=Z/8:PRINT A
1100 B%=(W-F)
1110 F=W
1120 *FX3,3
1130 VDU2
1140 PRINT "+";STR$(B%)
1150 GOTO 1210
1160 REM
1170 PRINTF:B%=ABS(W-F)
1180 *FX3,3
1190 VDU2
1200 PRINT"-";STR$(B%)
1210 *FX3,4
1220 VDU3
1230 F=W
1240 GOTO 345
1250 REM**************************
1260 REM*                        *
1270 REM*THE NEXT ROUTINE MAKES*
1280 REM*THE MONOCHROMATOR SCAN*
1290 REM*BETWEEN TWO SPECIFIED *
1300 REM*WAVELENGTHS           *
1310 REM*                      *
1320 REM**************************
1330 INPUT" Starting wavelength  (nm)",S:S=S*8
1340 INPUT" Finishing wavelength (nm)",F:F=F*8
1350 INPUT" Incremental rate "Inc
1360 P%=F-S:IF P%>=6400 THEN GOTO 1330
1370 IF P%<0 THEN GOTO 1330
1380 INPUT" Entrance slit (um)"S1
1390 INPUT" EXIT slit (um)"S2
1400 INPUT" PMT slit (um)"S3
1410 INPUT" Send to ADC or Chart A/C",a$
1420  IF a$="C" THEN PROCCHART
1430 CLS
1440 X=0
1450 P1=(F-S)/(Inc*8)
1460 FOR i=1 TO P1
1470 *FX3,3
1480 PRINT "+";STR$(P%/P1)
1490 *FX3,4
1500  PROCDATA
1510 FOR L1=1 TO 100:NEXT
1520 *FX21,1
1530 NEXT i
1540 *FX3,4
```

```
1550 PROCSAVE:PROCDRAW:GOTO 310
1560 REM MANUAL SCAN
1570 REM*************************
1580 REM*                       *
1590 REM*THE NEXT SEGMENT ALLOWS*
1600 REM*MANUAL SCAN            *
1610 REM*                       *
1620 REM*************************
1630 PRINT "To scan forward press "CHR$(93)
1640 PRINT:PRINT:PRINT "To scan backward press "CHR$(91)
1650 PRINT:PRINT:PRINT" Press Q to finish"
1660 *FX4,1
1670 Q$=GET$
1680 IF Q$=CHR$(&89) THEN PROCFORWARD
1690 IF Q$=CHR$(&88) THEN PROCBACK
1700 IF Q$="Q" THEN PROCFINISH
1710 DEF PROCFORWARD
1720 V%=10
1730 *FX3,1
1740 PRINT "+";STR$(V%)
1750 *FX3,4
1760 GOTO 1670
1770 ENDPROC
1780 DEF PROCBACK
1790 P%=10
1800 *FX3,1
1810 PRINT "-";STR$(P%)
1820 *FX3,4
1830 GOTO 1670
1840 ENDPROC
1850 DEF PROCFINISH
1860 *FX4,0
1870 *FX3,4
1880 *FX21,0
1890 GOTO 345
1900 ENDPROC
1910 DEF PROCCHART
1920 *FX3,1
1930 PRINT "+";STR$(P%)
1940 *FX3,4
1950 GOTO 345
1960 ENDPROC
1970 VDU3
1980 CLOSE#0:A=&FCC0
1990 REM ***   Data points stored   ***
2000 REM ***      in array Y(D).    ***
2010 REM *******************************
2020 DEF PROCDATA
2030 a=0
2040 *FX3,4
2050 FOR I=1 TO 300
2060 A=&FCC0
2070 A?0=0:Y=((A?0)*16)+((A?1)DIV16)
2080 a=a+Y
2090 NEXT
2100 Y(i)=(a/300)
2110 MOVE X,Y(i)/2:DRAW X,Y(i)/2:X=X+1200/P1
2120 ENDPROC
```

```
2130 REM ************************************************
2140 DEF PROCSAVE
2150 S=S/8:F=F/8:
2160 PRINT:PRINT
2170 PRINT TAB(15)"INSERT DATA DISK"
2180 INPUT "Name of file  " B$:Y=OPENOUT(B$)
2190 FOR D=1 TO P1
2200 PRINT#Y,Y(D) :NEXT:CLOSE#0
2210 FOR i=1 TO P1
2220 IF Y(i)>YMAX THEN YMAX=Y(i)
2230 NEXT
2240 DEF PROCDRAW
2250 CLS
2260 X=50
2270 FOR I1=1 TO P1
2280 MOVE X,Y(I1)*900/YMAX+50
2290 DRAW X,Y(I1)*900/YMAX+50
2300 X=X+1100/P1
2310 NEXT
2320 VDU5
2330 MOVE 50,50:DRAW 1200,50:DRAW 1200,1000:DRAW 50,1000
2340 FOR I2=1 TO 4
2350 MOVE 50,237.5*I2:PRINT"-"
2360 NEXT
2370 MOVE 200,950:PRINT"Intensity vs Wavelength (nm) "
2380 REM F=1600:S=800
2390 B=(F-S)/(800)
2400 FOR I2=0 TO B
2410 MOVE 37+1150/((B))*I2,60:PRINT"|"
2420 NEXT
2430 @%=&10
2440 FOR I2=0 TO 2
2450 MOVE -420+(1150/((B)))*I2*(B/2),30:PRINT S+I2*(F-S)/
2460 NEXT
2470 VDU4
2480 PRINT TAB(3,5)"REPEAT SCAN Y/N"
2490 INPUT G$:IF G$="Y" GOTO 2510
2500 GOTO 190
2510 B%=(F-S)*8
2520 *FX3,3
2530 VDU2
2540 PRINT"-";STR$(B%)
2550 *FX3,4
2560 VDU3
2570 PRINT"PRESS ANY KEY TO REPEAT SCAN"
2580 K=GET
2590 F=F*8:S=S*8
2600 GOTO 1430
2610 END
```

Program 2

System Response Generation

```
 10 REM ****  program to generate  ***
 20 REM ****  system response      ***
 25 REM ****  BY C.POTTER          ***
 30 DIMA(660)
 40 DIMB(660)
 50 DIMC(660)
 60 DIMD(660)
 70 PROClamp
 75 PROClistlamp
 80 PROCsyslamp
 90 PROCdivide
100PROCnorm
110PROCsave
120END
130DEF PROClamp
140 FOR I=505 TO 585
150 A(I)=1.385E-2*I-5.19999
160 NEXT I
170ENDPROC
180 DEF PROCsyslamp
190 CLS:PRINT"ENTER FILENAME OF SYSTEM AND LAMP DATA":INPUTA$
200 Y=OPENIN A$
210 FOR I=505 TO 584
220 INPUT #Y,B(I)
230 NEXT I
240 CLOSE#Y
250ENDPROC
260DEF PROCdivide
270DMAX=-99
280FORI=505 TO 585
290D(I)=B(I)/A(I)
300IFD(I)>DMAX THEN DMAX=D(I)
310NEXT I
320ENDPROC
330DEF PROCnorm
340FORI=505 TO 585
350 C(I)=D(I)/DMAX
360 NEXT I
370ENDPROC
380DEF PROCsave
390CLS:PRINT"ENTER THE SYSTEM FILENAME":INPUT B$
400 X=OPENOUT B$
410 FOR I=505 TO 585
420 PRINT#X,C(I)
430 NEXT I
440 CLOSE#X
450 ENDPROC
460 DEF PROClistlamp
470 CLS:PRINT:PRINT:PRINT:PRINT"DO YOU WANT TO LIST THE LAMP
      IF F$="N"THEN 520
480 VDU2
490 PRINT"WAVELENGTH","INTENSITY"
500 FORI=505 TO 585:A(I)=1.385E-2*I-5.19999:PRINTA(I),I:NEXT I
510PRINT:PRINT"PRESS spacebar TO FINISH":W$=GET$
515 VDU3
520 ENDPROC
```